To the Graduate Council

I am submitting herewith a thesis written by Rodney Harvill entitled "Thermoacoustic Waves in Liquid Metal Targets for High Power Spallation Neutron Sources." I have examined the final copy of this thesis for form and content and recommend that it be accepted in partial fulfillment of the requirements for the degree of Master of Science, with a major in Nuclear Engineering.

Art E. Ruggles, Major Professor

We have read this thesis
And recommend its acceptance:

Accepted for the council:

Associate Vice Chancellor
And Dean of the Graduate School

THERMOACOUSTIC WAVES IN LIQUID METAL TARGETS FOR HIGH POWER SPALLATION NEUTRON SOURCES

A THESIS

Presented for the

Master of Science

Degree

The University of Tennessee, Knoxville

Rodney Harvill

May, 1999

ACKNOWLEDGEMENTS

Many people have contributed to my graduate work. I am grateful to the members of my thesis committee, Drs. Arthur Ruggles, J.A.M. Boulet, Peter Groer, Ronald Pevey and Lawrence Townsend for their support. I would especially like to single out Arthur Ruggles for thanks. As my adviser, he provided guidance without which I would not have been able to complete this Thesis.

I would like to thank Rusi Taleyarkhan and Lockheed Martin for sponsoring my graduate project and providing much needed financial support.

Finally, I cannot praise my wife enough. She provided me with support in more ways than I can count.

Rodney Harvill

ABSTRACT

The target of the Spallation Neutron Source (SNS) is subjected to bursts of protons lasting less than a microsecond that occur 60 times each second. Each Proton burst deposits thermal energy that causes a pressure distribution in the target. The evolution of this pressure distribution with time must be accurately simulated to facilitate a robust target design. The experimental facility described herein uses a one-dimensional waveguide to create fluid and fluid-structure interactions prototypic of those expected from the pressure wave propagation.

This experimental facility permits the collection of data that characterize the interaction of large amplitude pressure waves with various structures. Incident pressure waves exceeding 6.89 MPa (1000 psi) are possible in mercury with pulse widths less than one millisecond. Various materials are used to reflect these waves, and the effect of material properties and surface condition can be examined by observing variations in incident and reflected pressure waves. The facility provides data suitable for validation of the material physics codes used to simulate the SNS target response to the proton pulse deposition. Consequently, data from this experiment allows validation of the material physics code currently employed to simulate the SNS target response.

TABLE OF CONTENTS

CHAPTER		PAGE
I.	BACKGROUND	1
II.	FIRST ORDER EVALUATION OF TARGET RESPONSE TO ONE PROTON PULSE	3
III.	WAVEGUIDE DESIGN	7
	Waveguide Operation	7
	System Description	8
	System Operation	9
	Waveguide Construction	10
	Solenoid And Piston Assembly	13
	Pressure Measurement Devices	14
	Head And Drain Tanks	15
	Vacuum Pump	16
	Mercury containment Provisions	16
	Health And Safety	17
IV.	DATA ACQUISITION SYSTEM	18
V.	RESULTS IN WATER	21
VI.	RESULTS IN MERCURY	29
VII.	CONCLUSIONS	31
VIII	FUTURE WORK	32
REFERENCES		34
APPENDIX		
A.	DERIVATION OF MECHANICAL WORK FROM EXPANSION OF AFFECTED VOLUME	37
B.	DERIVATION OF SOUND SPEED AS A FUNCTION OF THE RATIO OF PIPING INNER DIAMETER TO WALL THICKNESS	42
C.	PRESSURE DROP CALCULATIONS	50
D.	ACOUSTIC BOUNDARY ANALYSIS	56

APPENDIX		PAGE
E.	BRANCH ANALYSIS	61
	Acoustic Branch	62
	Helmholz Oscillators	64
F.	HYDRAULIC ACCUMULATOR SCOPING CALCULATIONS	70
G.	TRANSDUCER SPECIFICATIONS	75
H	WAVEGUIDE EXPERIMENTAL DESIGN AND PLANNING REPORT	77
I	DOCUMENTATION OF DATA	98
J	TIME OF FLIGHT	109
K	PICTURES OF WAVEGUIDE	114
NOMENCLATURE		119
VITA		121

LIST OF TABLES

TABLE		PAGE
1.	Waveguide Sound Speed As A Function Of Boundary Condition	12
C-1.	Pressure Drop Information For The Tubing In The Waveguide System	54
C-2.	Pressure Drop Information For The Fittings In The Waveguide System	55
E-1.	Acoustic Branches	68
I-1	Parameters Used For Cases With Water In The Waveguide	101
I-2	Parameters Used For Cases With Mercury In The Waveguide	107
J-1	Sound Speed Associated With Each Water Case	111
J-2	Sound Speed Associated With Each Mercury Case	113

LIST OF FIGURES

FIGURE		PAGE
1.	Drawing Of The Waveguide	8
2.	Drawing Of The Waveguide Piping System	9
3.	Diagram Of The Solenoid Control Circuit	15
4.	Diagram Of The Data Acquisition System With Water In The Waveguide	18
5.	Diagram Of The Data Acquisition System With Mercury In The Waveguide	20
6.	Water Data Taken With Rubber Impact Diaphragm, 0.4-Inch Stainless Steel Coupon (Blind Flange), No Flow In Waveguide, Transducer 1 In Port P1, Transducer 2 In Port P3, First Data File In Set	22
7.	Water Data Taken With Rubber Impact Diaphragm, 0.4-Inch Stainless Steel Coupon (Blind Flange), No Flow In Waveguide, Transducer 1 In Port P1, Transducer 2 In Port P3, Fifteenth Data File In Set	22
8.	Water Data Taken With Rubber Impact Diaphragm, 0.025-Inch Stainless Steel Coupon, No Flow In Waveguide, Transducer 1 In Port P1, Transducer 2 In Port P3	23
9.	Water Data Taken With 0.010-Inch Stainless Steel Impact Diaphragm, 0.025-Inch Stainless Steel Coupon, No Flow In Waveguide, Transducer 1 In Port P1, Transducer 2 In Port P3	23
10.	Water Data Taken With 0.025-Inch Stainless Steel Impact Diaphragm, 0.025-Inch Stainless Steel Coupon, No Flow In Waveguide, Transducer 1 In Port P1, Transducer 2 In Port P3	24
11.	Water Data Taken With 0.063-Inch Stainless Steel Impact Diaphragm, 0.025-Inch Stainless Steel Coupon, No Flow In Waveguide, Transducer 1 In Port P1, Transducer 2 In Port P3	24
12.	Water Data Taken With Rubber Impact Diaphragm, 0.020-Inch Stainless Steel Coupon, No Flow In Waveguide, Transducer 1 In Port P1, Transducer 2 In Port P3	26

FIGURE		PAGE
13.	Water Data Taken With 0.063-Inch Stainless Steel Impact Diaphragm, 0.020-Inch Stainless Steel Coupon, 83 kPa (12 Psid) Across Waveguide, Transducer 1 In Port P1, Transducer 2 In Port P3	26
14.	Water Data Taken With Rubber Impact Diaphragm, 0.020-Inch Stainless Steel Coupon, 255 kPa (37 Psid) Across Waveguide, Transducer 1 In Port P1, Transducer 2 In Port P3	27
15.	Water Data Taken With Rubber Impact Diaphragm, 0.025-Inch Stainless Steel Coupon, No Flow In Waveguide, Transducer 1 In Port P1, Transducer 2 In Port P3	27
16.	Water Data Taken With 0.063-Inch Stainless Steel Impact Diaphragm, 0.025-Inch Stainless Steel Coupon, No Flow In Waveguide, Transducer 1 In Port P1, Transducer 2 In Port P2	28
17.	Mercury Data Taken With 0.025-Inch Impact Diaphragm And 0.010-Inch Reflection Coupon, No Flow In Waveguide	30
18.	Mercury Data Taken With 0.010-Inch Impact Diaphragm And 0.010-Inch Reflection Coupon, No Flow In Waveguide	30
A-1	Work Performed On The Target As A Result Of One Proton Pulse Given An Average Energy Deposition Rate Of One Megawatt	41
B-1.	Diagram Of The Control Volume At Time t And At Time $t + dt$	44
B-2.	Sound Speed In Mercury In The Waveguide	49
D-1.	Diagram Of The Forces Associated With An Acoustic Boundary	58
E-1.	Diagram Of A Side Connection	62
E-2.	Diagram Of A Helmholz Resonator	66
E-3.	Transmissivity Of The Transducer Port As A Function Of Incident Pressure Wave Frequency	68
E-4.	Reflectivity Of The Transducer Port As A Function Of Incident Pressure Wave Frequency	69
K-1	Waveguide And Vacuum Pump	115

FIGURE PAGE

K-2 Solenoid And Impact Diaphragm 115

K-3 Reflection Coupon 116

K-4 Mercury Transfer Pump 116

K-5 Hydraulic Accumulators 117

K-6 Head Tank 117

K-7 Drain Tank 118

CHAPTER I

BACKGROUND

The National Spallation Neutron Source (SNS) is a pulsed proton accelerator with a liquid mercury target. This target is subjected to bursts of protons lasting less than a microsecond that occur 60 times each second. When protons in the particle beam strike the nuclei of the mercury in the target, neutrons are dislodged. These neutrons are subsequently used for neutron scattering experiments. A detailed description of the SNS is given in it's the "National Spallation Neutron Source Conceptual Design Report" (Oak Ridge National Laboratory 1997).

The proton pulse deposits thermal energy in the mercury target volume over a period of roughly one half microsecond. The volume of mercury in the target experiencing spallation is heated by the pulse during this time. The abrupt change in enthalpy of the mercury causes an abrupt change in the pressure distribution of the target. The pressure propagation velocity in the mercury is roughly 1,450 m/s, so the pressure information moves less than one millimeter during the time the energy is deposited. Therefore, the pressure field initially established by the pulse is spatially similar to the energy deposition field. The peak pressure in this field is over 10 MPa. The pressure boundary may be subjected to cavitation, plastic deformation and fatigue attributable to the pressure wave motivated by the incident proton bursts. These responses should be carefully considered to facilitate a robust target design.

The evolution of the pressure field with time after the proton pulse will be predicted and the quasi-steady response of the target to the periodic application of proton pulses will be simulated as part of the current SNS target development plan. This

includes modeling in the mercury and modeling of fluid structure interactions. A number of material physics codes are being used to predict the response of the target to the incident pressure waves caused by the proton pulses. The most promising code is CTH (McGlaum and Thompson 1990). The experimental facility described herein allows the performance of the material physics code to be validated in a simple geometry that employs materials prototypic of the SNS target. Note that the validation of the code is to be performed at a later date and is not discussed here.

The experimental facility includes a stainless steel tubular waveguide with wall thickness 0.0075 meter and inner diameter 0.0064 meter and length 3.9 meters. The waveguide is fitted with a diaphragm at one end that is struck with a piston to create pressure waves in the fluid. Pressure measurement devices are positioned along the waveguide and the end opposite the diaphragm is fitted with a flange onto which blanks of any desired material can be attached. Thus, the fluid-structure response of materials with different mechanical and surface characteristics can be examined.

The fluid can be circulated through the waveguide at velocities up to 1.44 m/s and the waveguide can be pressurized to 1.2 MPa. Many elements lighter than mercury are formed as a result of the nuclear spallation reaction. Therefore, the composition of the target material will change slowly during operation of the facility. The mercury can be contaminated to simulate the effects of prolonged operation on the measured pressure wave propagation. The simple one-dimensional geometry is easy to model, allowing the validation of the CTH code to focus on the physics of the fluid and fluid-structure interactions. Data from the facility can also be used to extend the models in the CTH code where this is required to enhance the fidelity of the simulation.

CHAPTER II

FIRST ORDER EVALUATION OF TARGET RESPONSE TO ONE PROTON PULSE

A first order evaluation of how pressure waves are created by the incident proton pulse is presented here. This development motivates the physics to be evaluated with the experimental facility.

Each proton pulse deposits 16.7 kJ over a one-half-microsecond time period. This energy deposition causes the following near constant volume change in temperature:

$$Q = mc_v \Delta T, \qquad [2\text{-}1]$$

where c_v is the specific heat for a constant volume process, Q is the amount of energy deposited and m is the mass of the material in which the energy, Q, is deposited.. The target is a liquid, and therefore the value for c_v is very near to the value for c_p. The mercury volume does not change significantly during the deposition of energy by the proton pulse because the pressure wave speed in mercury limits the pressure wave motion to less than 1 millimeter during the pulse. Therefore, the spatial energy distribution from the pulse produces a similar spatial pressure distribution.

Changes in pressure and work caused by one proton pulse are approximated starting with the sound speed equation,

$$c^2 = \frac{dP}{d\rho}, \qquad [2\text{-}2]$$

where the process line for the application of the derivative is yet to be established. In this case, pressure is taken as a function of temperature and density,

$$P = P(\rho, T). \qquad [2\text{-}3]$$

Because pressure is a function of both temperature and density, its derivative is

$$dP = \frac{\partial P}{\partial \rho} d\rho + \frac{\partial P}{\partial T} dT . \qquad [2\text{-}4]$$

For a constant volume or density heat-up, the derivative becomes

$$dP = \frac{\partial P}{\partial T} dT . \qquad [2\text{-}5]$$

The process line for the derivative in [2-2] is normally taken to be isentropic. However, the compressibility of a liquid is insensitive to the process line since c_p is near to c_v. Hence, the sound speed equation can be rewritten as

$$dp = c^2 \left[dT \frac{d\rho}{dT} \right]. \qquad [2\text{-}6]$$

The constant volume heat-up of mercury is followed by an adiabatic expansion process, which transfers energy to the surrounding material in the form of a pressure wave. This energy transfer is defined as

$$W = \int p dV . \qquad [2\text{-}7]$$

Applying the following definition,

$$V = \frac{m}{\rho}, \qquad [2\text{-}8]$$

and taking the first derivative of the expression, assuming that mass, m, is constant, gives

$$dV = -m \frac{d\rho}{\rho^2} . \qquad [2\text{-}9]$$

Define the total change in temperature due to the proton pulse as δT and the total change in pressure as δp. Equation [2-9] is substituted into [2-7] to form

$$W = -\frac{V^2}{2mc^2} \delta p^2 , \qquad [2\text{-}10]$$

where

$$\delta p = c^2 \delta T \frac{d\rho}{dT}. \qquad [2\text{-}11]$$

Note that all non-linear effects have been ignored. Thus, the work performed on the surrounding target material during the adiabatic expansion is

$$W = -\frac{V^2 c^2}{2m}\left(\frac{Q}{mc_v}\frac{d\rho}{dT}\right)^2. \qquad [2\text{-}12]$$

Equation [2-12] shows that the mechanical work performed on the target during the adiabatic expansion is 356 J if all the proton pulse energy is dissipated in a 100 cubic centimeter volume and 697 J if all the proton pulse energy is dissipated in a 50 cubic centimeter volume. From [2-11], the pressure changes associated with the two volumes over the course of the heat-up are 450 MPa and 890 MPa, respectively. Note that the amount of mechanical work is very small relative to the amount of incident thermal energy, which is consistent with the assumption that the ratio of specific heats is near unity. More details from this evaluation are available in Appendix A.

The volume of mercury in the target must increase by 1.6 cubic centimeters to relax the pressure created by a single proton pulse. This roughly represents the amount of mercury volume expansion the SNS target pressure boundary must accommodate after each pulse if dynamic effects are neglected. This increase in volume is the same regardless of the size of the volume in which the pulse energy is dissipated when dynamic and nonlinear effects are ignored. Therefore, the difference in the calculated mechanical work values is entirely a function of the peak pressure, or initial pressure

distribution caused by the pulse. The volume change required to relax the pressure is a function of the energy deposition.

The pressure waves will intersect the pressure boundary used to contain the liquid mercury. This boundary is currently of stainless steel construction with walls of nominally 0.003 meter thickness.

The interaction of the wave with the stainless steel boundary must be well understood to allow design of a target that can achieve acceptable performance. The target must be reliable and endure service for several months prior to replacement if current availability goals for the SNS facility are to be attained.

CHAPTER III

WAVEGUIDE DESIGN

When a pressure wave is generated in a waveguide, it propagates down the waveguide, and its magnitude is measured by transducers placed along the length of the waveguide. At the end of the waveguide, the pressure wave reflects and propagates in the opposite direction along the waveguide. Again, its magnitude is measured by the same transducers. Given an incident wave profile and characteristics of a reflection coupon, a material physics code predicts the profile of the reflected wave. The predicted wave profile can be compared to the measured wave profile to benchmark the code's performance.

A waveguide/shock tube has been constructed to allow studies of pressure wave performance in mercury contained in stainless steel. The facility is shown in Figure 1 and consists of a waveguide with a diaphragm at one end that can be struck with a piston to create pressure pulses. The opposite end of the waveguide has a flange onto which material coupons can be attached. These coupons can have different structural and surface properties to establish the relationship between these properties and the fluid-structure response. The waveguide is fitted with two pressure transducers. There are three locations where these transducers can be mounted denoted by P1, P2 and P3 in Figure 1.

Waveguide Operation

A pressure pulse is formed within the waveguide when the piston is driven by spring force into the diaphragm at one end of the waveguide. This pressure pulse propagates down the waveguide and is measured by the pressure transducers as it passes

their positions. When the pressure wave reaches the coupon at the opposite end of the waveguide, part of the wave reflects and propagates in the opposite direction down the waveguide. The reflected pulse is measured by the pressure transducers as it moves towards the diaphragm. The difference between incident and reflected waves can thereby be measured.

System Description

The system supporting the waveguide, shown in Figure 2, consists of two tanks and a mercury transfer pump. This system has been designed to permit testing both when the mercury is stationary within the waveguide and when it is flowing through the waveguide. The head tank provides driving head for gravity induced flow through the

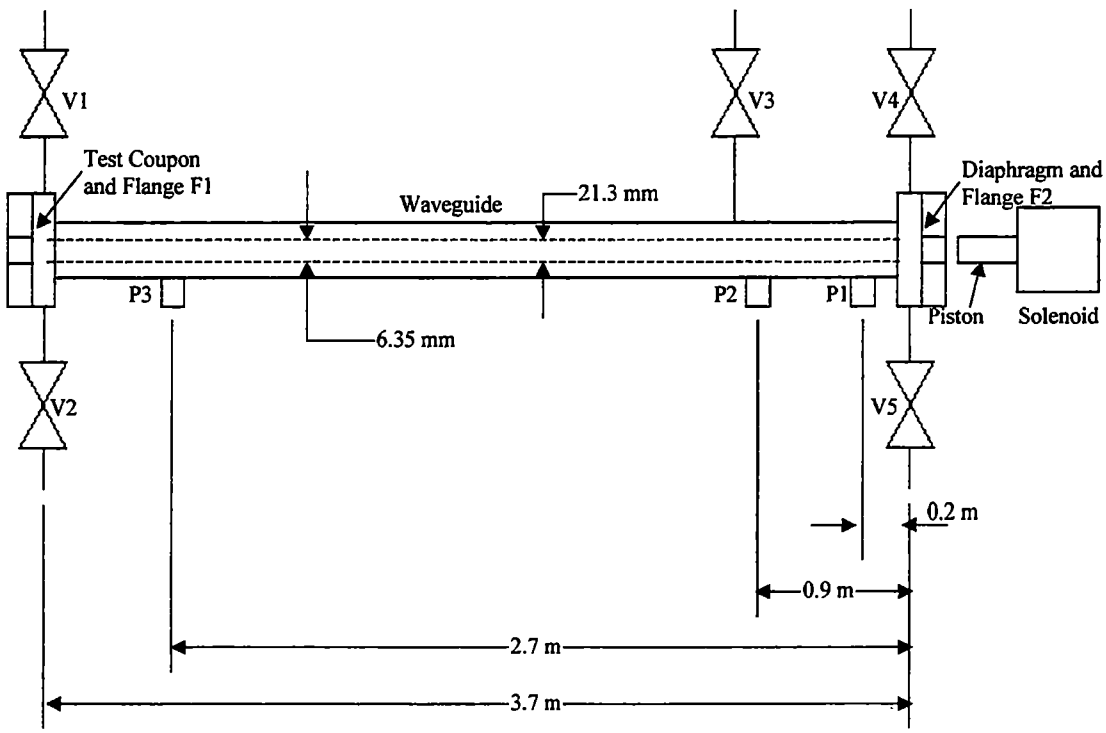


Figure 1 – Drawing Of The Waveguide. V1 Through V5 Are Packless Stainless Steel Valves. P1, P2, and P3 Are Transducer Locations

waveguide, allowing tests under flowing conditions. The drain tank is used to collect the mercury when the waveguide is vented or drained and serves as the reservoir to which the mercury flows when testing is performed under gravity-driven flow conditions. The mercury transfer pump is used to move mercury from the drain tank to the head tank and to circulate mercury through the waveguide. The mercury transfer pump is a positive displacement diaphragm pump, and its discharge is pulsed and causes pressure oscillations. Because these pressure perturbations would complicate pressure pulse studies in the waveguide, hydraulic accumulators are located on the suction and discharge of the mercury transfer pump to smooth the flow and pressure oscillations. The accumulators are sized based on calculations given in Appendix F. The flow in the

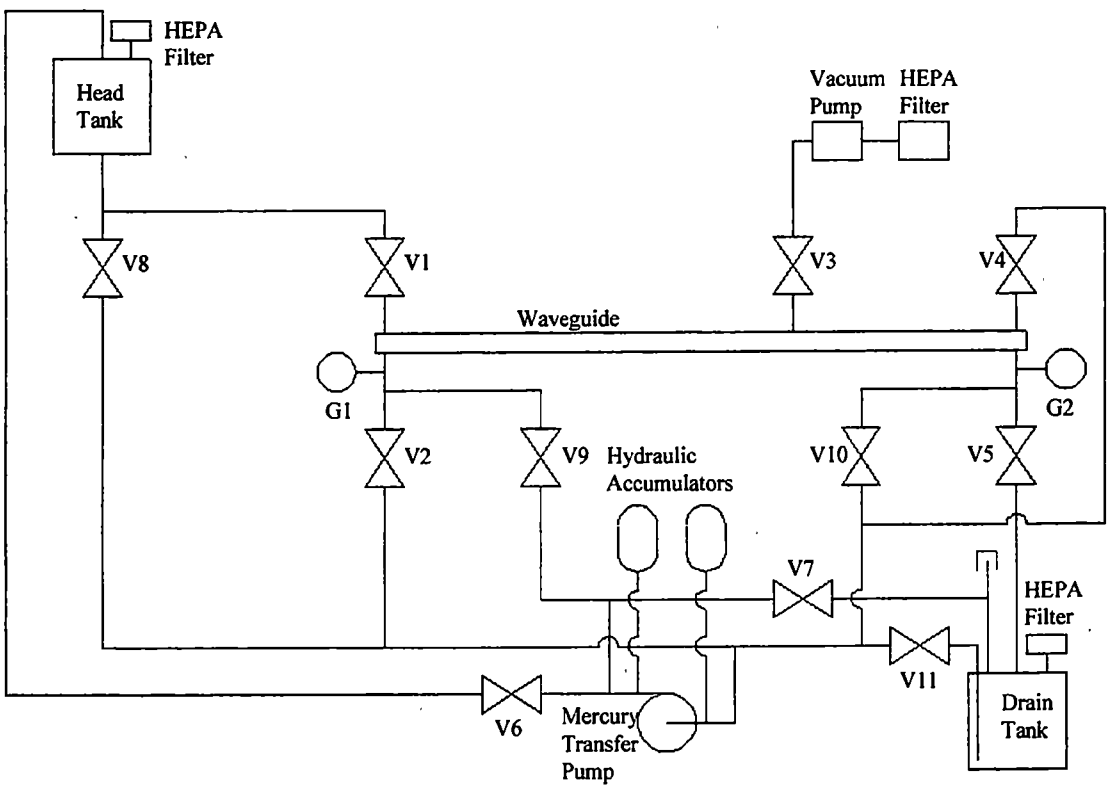


Figure 2 – Drawing Of The Waveguide Piping System. V1 Through V11 Are Packless Stainless Steel Valves. G1 And G2 Are Pressure Gages.

waveguide can be governed by gravity and valve position or by the operation of the transfer pump in conjunction with valve position. Photographs of the components of the waveguide are located in Appendix K.

System Operation

The flow through the waveguide can be driven by gravity or by the mercury transfer pump. When gravity-driven flow is employed, mercury flows from the head tank through valve V1 into the waveguide. The mercury then flows out of the waveguide through valve V5 into the drain tank. The mercury transfer pump draws suction on the drain tank through valve V11 and pumps the mercury back to the head tank via valve V9. When the transfer pump is used to drive the flow through the waveguide, only a portion of the pump's fixed flow-rate is directed through the waveguide. The rest of the flow is directed to the head tank. When mercury leaves the discharge of the transfer pump, some of the flow is directed through valve V6 into the waveguide. The mercury then flows out of the waveguide through valve V10 back to the suction of the transfer pump. The rest of the flow is directed through valve V9 to the head tank. From the head tank, the mercury flows through valve V8 back to the suction of the pump.

Waveguide Construction

The waveguide is constructed from 3.7 meters of one-half-inch schedule XXS stainless steel (316) tubing, which has an inner diameter of 0.0064 m and a wall thickness of 0.0075 m (Nayyar 1992, E.14). The purpose of such thick-walled tubing is to provide a rigid boundary condition for waves passing through the fluid in the waveguide. While the typical sound speed calculation for fluid in a pipe assumes a rigid boundary condition, real pipes are not perfectly rigid. Consequently, the flexibility of the pipe wall affects the

sound speed in the combined fluid and pipe system. The theoretical sound speed in bulk mercury is roughly 1450 m/s. Calculations have been performed to determine the sound speed in the mercury in the waveguide when the pressure vessel walls are elastic and subject to the following boundary conditions (Parmakian 1963, 19):

(a) a tube fixed at one end, free to move longitudinally throughout its length and without expansion joints.

(b) a tube anchored against longitudinal movement throughout its length.

(c) a tube fixed at both ends with expansion joints throughout its length.

It should be noted that these calculations consider only the first mode of an infinite number of modes (Scarton 1973).

When the stainless steel pressure vessel is infinitely thick, the wall elasticity is minimal and the predicted sound speed is at a maximum. Table 1 shows the sound speed in mercury in an infinitely thick pressure vessel and for the mercury in the waveguide, which has an inner-diameter-to-wall-thickness ratio of 0.857, for the three boundary conditions previously described. It should be noted that the sound speed in mercury is signficantly reduced even for the infinitely thick wall case. This is attributable to the low compressibility of mercury. Details of this evaluation are given in Appendix B.

While all three cases are idealized conditions, the one most applicable to the waveguide is case (c) because the waveguide is restrained by elastic shock mounts throughout its length. For this case, the sound speed for the waveguide is 1131 m/s representing a 22% reduction in sound speed compared to that for bulk mercury. The 0.252-inch inner diameter of the waveguide minimizes the inventory of mercury in the waveguide. Because mercury is a hazardous material, it is desired to minimize its

inventory at the test site. As a result of the small volume of the waveguide, 1.3×10^{-4} cubic meters, only 1.7 kilograms of mercury must be in the waveguide during testing. The small diameter permits temporal resolution of wavelengths down to five centimeters, corresponding to 23 kHz. This resolution is adequate for time of flight measurements and permits a plane wave assumption in the waveguide for these wavelengths. When a wave passes through small-diameter tubing, it causes fluid motion near the walls that can cause viscous dissipation of energy according to the following equation (Kinsler and Frey 1962, 238-40):

$$P = P_0 e^{-\alpha x}, \qquad [3\text{-}1]$$

where

$$\alpha = \frac{1}{ac}\sqrt{\frac{\eta\omega}{2\rho_0}} \qquad [3\text{-}2]$$

and

$$\omega = 2\pi f . \qquad [3\text{-}3]$$

For [3-2], the shear coefficient of viscosity, η, in mercury is 0.0016 Ns/m^2, and the frequency, f, is 15 kHz. The density, ρ, of mercury is 13, 600 kg/m^3. This energy

Table 1 – Waveguide Sound Speed As A Function Of Boundary Condition

Boundary Condition Case	Sound Speed (m/s)		
	Infinitely thick walls	Waveguide	Bulk Mercury
a	1296	1223	1450
b	1307	1263	1450
c	1218	1131	1450

dissipation causes a 7% reduction in pressure amplitude for a wave travelling the 7.4 meters from the impact diaphragm to the reflection coupon and back to the impact diaphragm. Note that orifice plugs are used in the fill and drain lines near the waveguide to minimize acoustic loses into these branches.

The 3.7-meter length of the waveguide permits reasonable temporal resolution of long wavelengths. The distance between transducer locations P1 and P3 in Figure 1 is 2.5 m, permitting resolution for frequencies as low as 505 Hz. The distance between transducer location P3 and the reflection assembly is 0.97 m. Therefore a wavelength of 1.94 m, corresponding to a frequency of 651 Hz, can be resolved without interference of both the incident and reflected wave at the transducer.

The waveguide reflection assembly consists of a blind flange with a 1.9-cm hole drilled through it. This facilitates the placement of coupons of different materials or different thicknesses of the same material at the end of the waveguide where the waves reflect. This permits the study of the effect of material composition or thickness on the character of the reflected wave. The compliance of the material determines the phase of the reflected wave with respect to the incident wave.

Solenoid and Piston Assembly

A solenoid is used to hold the piston that forms the pressure pulse in the waveguide. When current is initiated to the solenoid, the piston retracts into the solenoid. When the current is interrupted, a spring drives the plunger into the diaphragm at the end of the waveguide. As the diaphragm is pushed forward, it displaces a volume of fluid, initiating the pressure wave. The plunger has a teflon tip designed to distribute the

impact forces evenly over the surface of the diaphragm. This arrangement is designed to produce a well-defined shock wave.

At equilibrium, the spring on the solenoid plunger is 11.4 cm long. At maximum compression, the spring is 2.5 cm. When the plunger is in contact with the impact diaphragm, the spring is compressed to a length of 10.2 cm. The maximum energy that the solenoid can transmit into the waveguide is calculated by means of

$$E = \int_{x_2}^{x_2} kx\,dx = \frac{1}{2}k\left(x_2^2 - x_1^2\right). \qquad [3\text{-}4]$$

Here, x_1 is 1.3 cm, and x_2 is 8.9 cm. The spring constant k is 1.56 kN/m. The calculated energy is 1.36 J.

The solenoid control system, shown in Figure 3, consists of a power supply, a push-button on/off switch, a relay, and the solenoid. When the switch is closed, current from the power supply energizes the relay. The relay then closes the circuit that powers the solenoid. When the solenoid is energized, its plunger retracts against spring compression into the solenoid body. When the switch is opened, the relay is deenergized. This causes the solenoid to lose power, and the spring pushes the plunger into the impact diaphragm. This system was designed to facilitate automation of the formation of pressure waves to allow averaging of many signals, if required.

Pressure Measurement Devices

The pressure waves in the waveguide are detected and measured by means of two PCB 102A04 piezoelectric transducers (PCB Piezotronics). Each transducer has a frequency response of greater than 500 kHz and is designed for shock wave detection. The specifications for these transducers can be found in Appendix G. The actual

measurement frequency response is limited to 34 kHz because that is the natural frequency of the pressure ports in which the transducers are installed. The frequency response of the pressure ports is developed in Appendix E. The positions of the three pressure transducer locations are shown in Figure 1.

Two stainless steel 0-300 psi pressure gauges are installed in the system, one at each end of the waveguide. They are used to monitor system pressure in the waveguide and serve as an indirect measurement of flow velocity in the waveguide.

Head and Drain Tanks

The facility utilizes two stainless steel tanks as indicated in Figure 1, both of which are made of stainless steel to prevent corrosion. Either the head tank, with a capacity of three gallons, or the drain tank, with a capacity of one gallon, can store the 40 kilograms of mercury in the system. The head tank holds 7.4 kilograms of mercury per

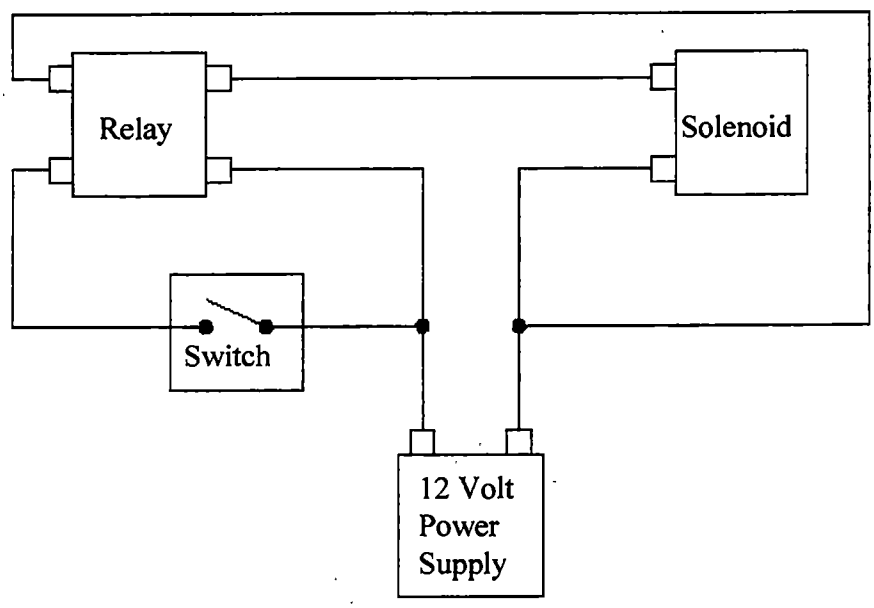


Figure 3 – Diagram Of The Solenoid Control Circuit

centimeter of height. This tank allows a near steady gravity driven flow rate in the system for 20 seconds. The drain tank has a capacity of 4.7 kilograms of mercury per centimeter, providing mercury to cover the suction line to the transfer pump. Both tanks have lexan lids that permit visual monitoring of the level of mercury in each tank. Each lid is equipped with a penetration for a Survivair HEPA filter whose purpose is to filter mercury vapor from air displaced in the tank as mercury flows from one tank to another. All other leak paths for air, such as tubing penetrations in the lids and the seams where the lids rest on the tanks, are sealed.

Vacuum Pump

A vacuum pump is used to evacuate air from the waveguide before it is filled with mercury. If air is present in the waveguide during testing, experimental results are distorted by the presence of additional compressibility in the system.

Mercury Containment Provisions

Because the system contains mercury, a hazardous material, it is important that it not leak. The ends of the waveguide are sealed by means of flanged fittings. All tubing connections use compression fittings. Threaded connections are kept to a minimum. Threaded connections are used at the mercury transfer pump inlet and outlet fittings, the pressure transducer ports, the pressure gauges, and the accumulators. The pump inlet and outlet fittings are NPT thread to Swagelock compression fitting adapters. The pressure transducer ports are sealed by means of brass seal rings. All threaded connections are sealed by means of teflon tape. The system contains eleven valves. These valves are packless and are connected to the rest of the system through compression fittings. The mercury transfer pump is a diaphragm pump. Both the head

and drain tanks are equipped with covers on which HEPA filters are mounted. These HEPA filters prevent mercury vapors from escaping into the atmosphere. The vacuum pump discharges through a HEPA filter. Drip trays are placed underneath the test facility to contain any leakage of mercury that may occur.

Health and Safety

The facility was delivered to Oak Ridge National Laboratory for testing with mercury. A waveguide Experimental Design and Planning Report was prepared and distributed to Oak Ridge National Laboratory Health and Safety personnel for approval prior to operation of the facility. A final approved version of this report is given in Appendix H.

CHAPTER IV

DATA ACQUISITION SYSTEM

A diagram of the data acquisition system for collection of data in water is shown in Figure 4. When a pressure pulse propagates through the waveguide, it is detected by two PCB 102A04 pressure transducers (PCB Piezotronics). The pressure transducers produce a voltage output that is transmitted to the signal conditioners by means of coaxial cables. These signal conditioners filter and amplify the signals before sending them to a National Instruments AT-5102 digital oscilloscope card. The card, which can support two channel operation and triggering, sends the signals to the 486 computer in which it is installed. National Instruments Virtual Bench software is the user interface to collect and

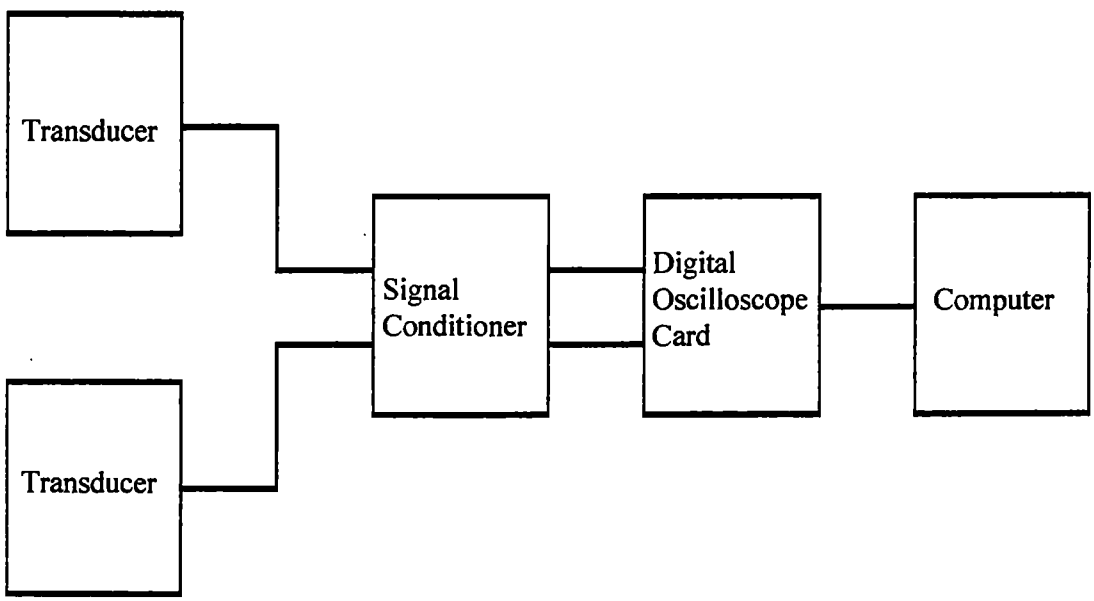


Figure 4 – Diagram Of The Data Acquisition System With Water Is In The Waveguide

store data on the computer's hard drives.

When mercury is in the system, the pressure pulses are greater than the 6.89 MPa (1000 psi) range of the PCB 102A04 pressure transducers. For the transducers, a 0 MPa pressure corresponds to a signal of 0 V. A 6.89 MPa pressure corresponds to a signal of 5 V. To exceed the 6.89 MPa pressure range of the transducers results in a signal of greater than 5 V. A verbal communication with PCB Piezotronics on September 2, 1998, confirmed that the 102A04 can safely exceed its 6.89 MPa pressure range. Its accuracy under this condition is within ±2%. The AT-5102 digital oscilloscope, however, can detect a maximum voltage range of ±5V. For the full pressure signal to be detected when mercury is in the system, a 10x probe is installed between the signal conditioner and the AT-5102, as shown in Figure 5. For this arrangement, a voltage output of 0.5 V corresponds to a pressure of 6.89 MPa.

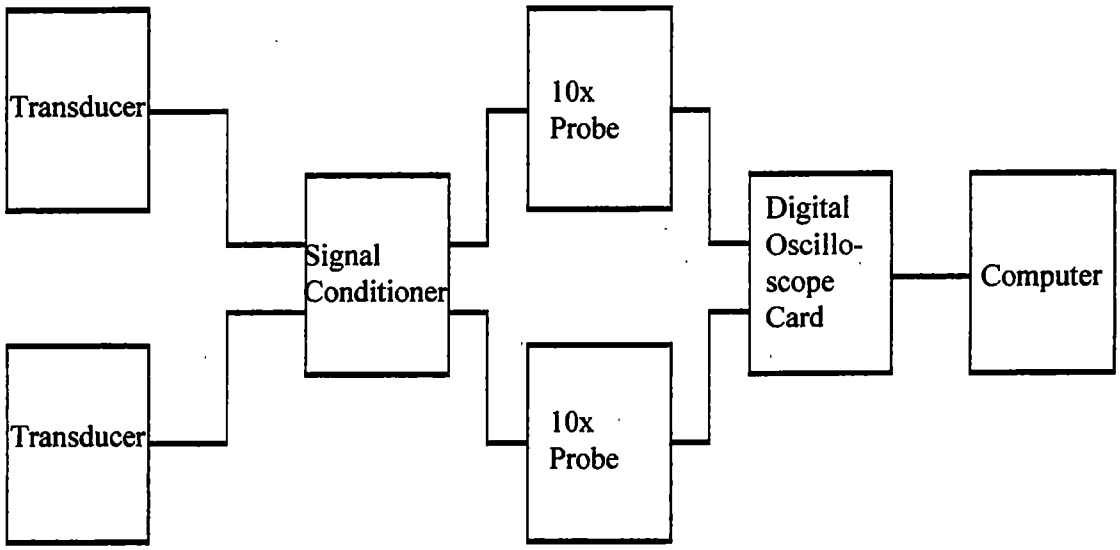


Figure 5 – Diagram Of The Data Acquisition System With Mercury In The Waveguide

CHAPTER V

RESULTS IN WATER

Pressure wave data was first collected with water in the waveguide. It was desired to do shake-down testing with water in the system to verify proper operation prior to loading mercury into the system. The first data sets were taken before a vacuum pump was added to the system. Figure 6 is the first data file from a data set collected with water in the system. Figure 7 is the fifteenth data file. Between data files fourteen and fifteen, the system was vented. The change in the pressure profile indicates that air was in the system. A vacuum pump was installed to remove air from the system prior to filling.

Figures 8, 9, 10 and 11 represent water data taken with the following impact diaphragms, respectively: rubber sheet, 0.010-inch stainless steel, 0.025-inch stainless steel and 0.063-inch stainless steel. In all four cases, the reflection coupon was 0.025-inch stainless steel. For the first case, a rubber sheet impact diaphragm, the pulse width generated by the impact of the piston against the diaphragm was one millisecond. For the next case, 0.010-inch stainless steel impact diaphragm, the pulse width was 0.7 millisecond. For the last two cases, 0.025-inch and 0.063-inch impact diaphragms, the pulse width was 0.6 millisecond. For stainless steel impact diaphragms, the thickness of the material has a minor effect. To obtain a shorter pulse width, the impact tip on the piston must be made of a material with an elastic modulus greater than teflon or the mass of the piston must be reduced. However, no effort was made to vary these properties in these studies.

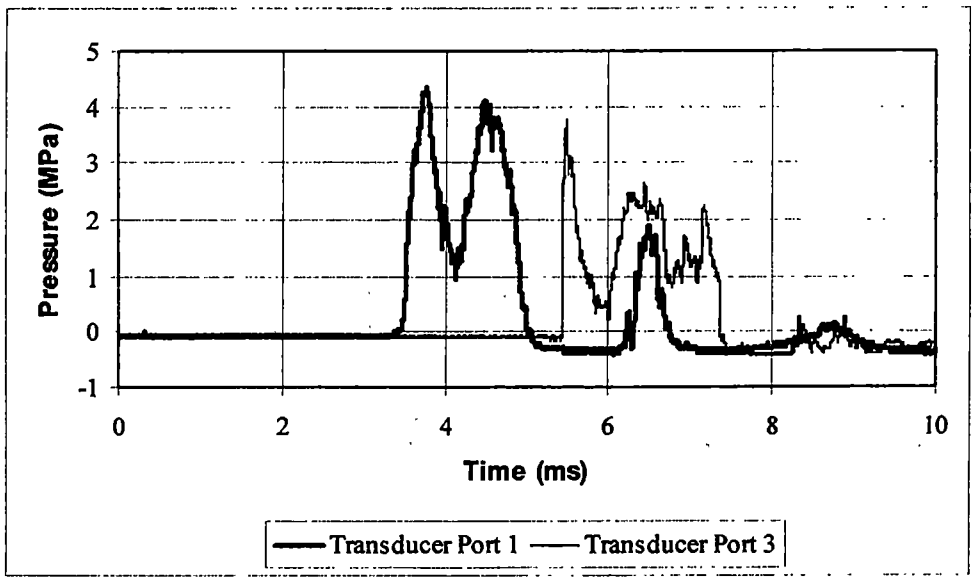


Figure 6 – Water Data Taken With Rubber Impact Diaphragm, 0.4-Inch Stainless Steel Coupon (Blind Flange), No Flow In Waveguide, Transducer 1 In Port P1, Transducer 2 In Port P3, First Data File in Set

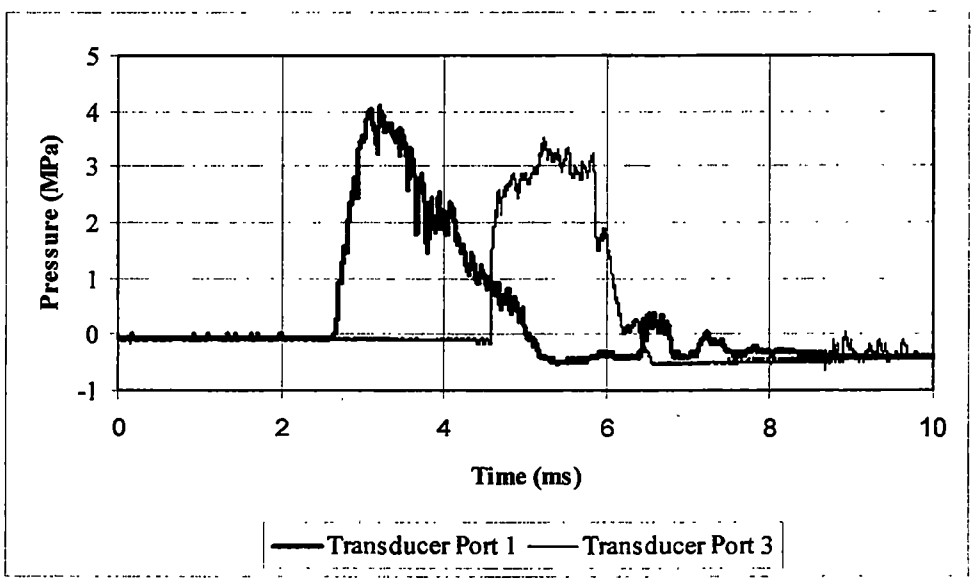


Figure 7 – Water Data Taken With Rubber Impact Diaphragm, 0.4-Inch Stainless Steel Coupon (Blind Flange), No Flow In Waveguide, Transducer 1 In Port P1, Transducer 2 In Port P3, Fifteenth Data File In Set

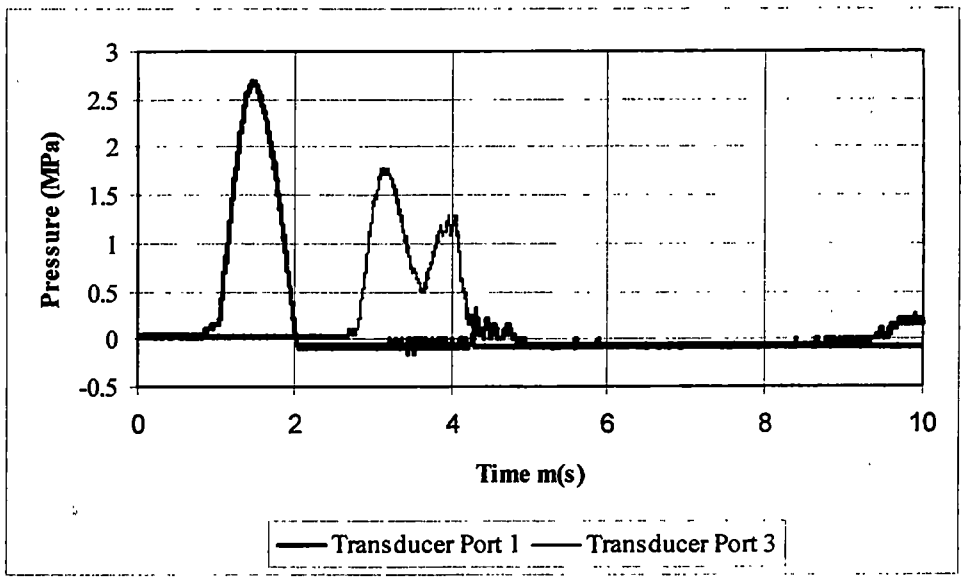


Figure 8 – Water Data Taken With Rubber Impact Diaphragm, 0.025-Inch Stainless Steel Coupon, No Flow In Waveguide, Transducer 1 In Port P1, Transducer 2 In Port P3

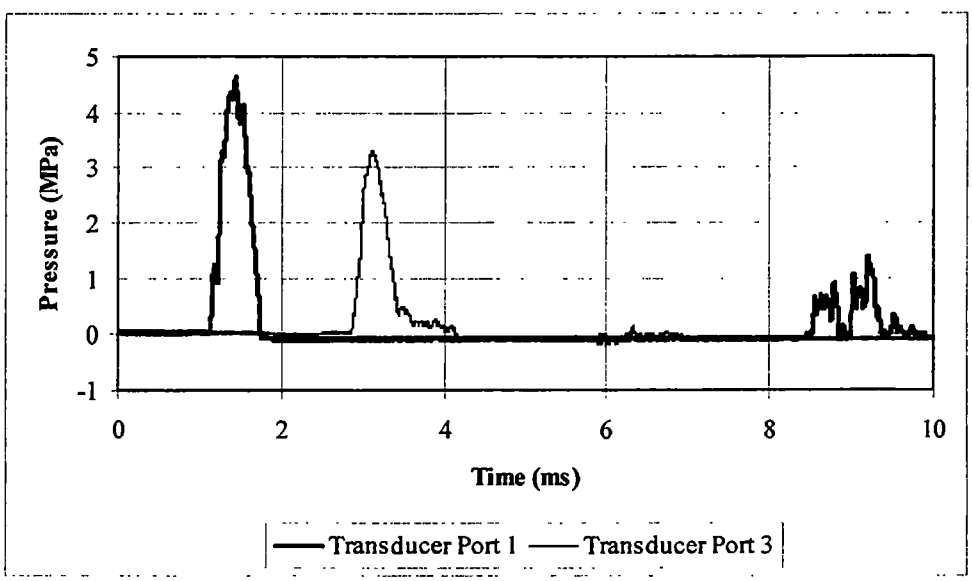


Figure 9 – Water Data Taken With 0.010-Inch Stainless Steel Impact Diaphragm, 0.025-Inch Stainless Steel Coupon, No Flow In Waveguide, Transducer 1 In Port P1, Transducer 2 In Port P3

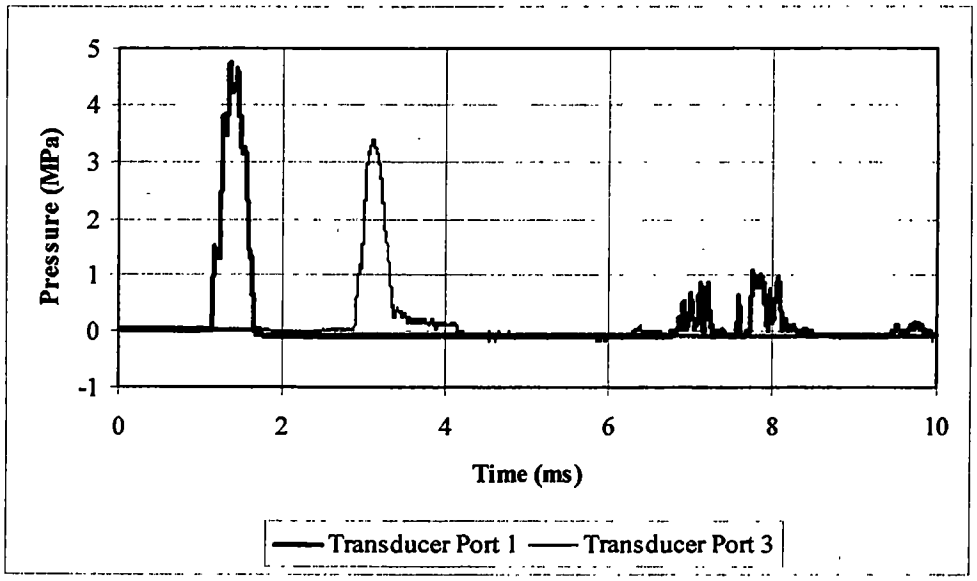


Figure 10 – Water Data Taken With 0.025-Inch Stainless Steel Impact Diaphragm, 0.025-Inch Stainless Steel Coupon, No Flow In Waveguide, Transducer 1 In Port P1, Transducer 2 In Port P3

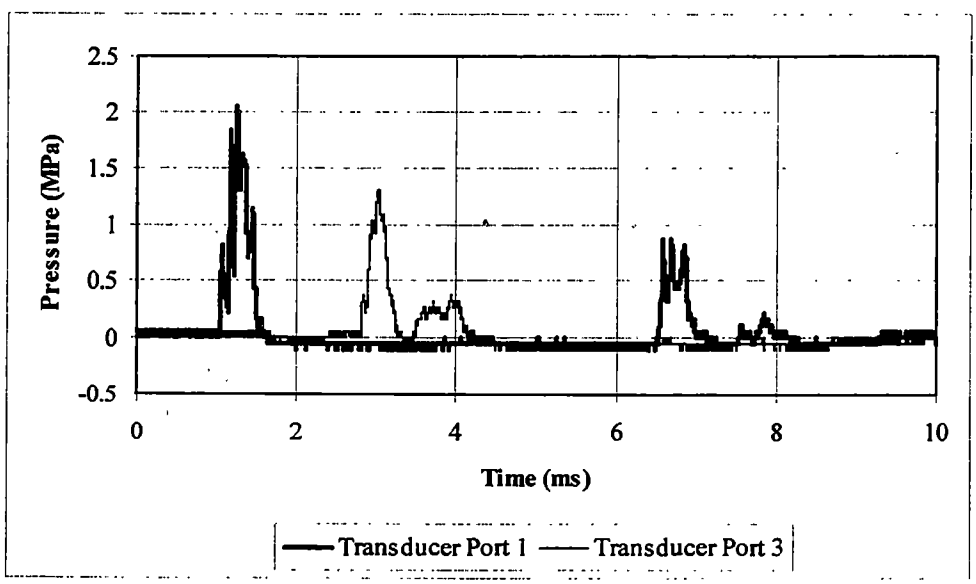


Figure 11 – Water Data Taken With 0.063-Inch Stainless Steel Impact Diaphragm, 0.025-Inch Stainless Steel Coupon, No Flow In Waveguide, Transducer 1 In Port P1, Transducer 2 In Port P3

Figures 12, 13 and 14 represent water data taken with a rubber sheet impact diaphragm and a 0.020-inch stainless steel reflection coupon. They represent the following flow conditions, respectively: no flow in the waveguide, flow with a 83 kPa (12 psi) pressure differential across the waveguide and flow with a 255 kPa (37 psi) pressure differential across the waveguide. In all three cases, there is a positive reflected wave. However, the reflected wave is more positive as the flow through the waveguide increases, as indicated by the increase in differential pressure across the waveguide.

Figures 15 and 16 represent water data taken with a 0.063-inch stainless steel impact diaphragm and a 0.025-inch stainless steel reflection coupon. In Figure 15, pressure data from ports 1 and 3 are represented. In Figure 16, pressure data from ports 1 and 2 are represented. The pressure wave has lost ten percent of its energy when propagating from port 1 to port 2 and forty percent of its energy when propagating from port 1 to port3. Theoretically, there should be a loss of energy of roughly twenty-three percent as the wave propagates from port 1 to port 3, accounting for viscous losses and losses at the vacuum pump connection. The loss of energy from port 1 to port 2 should be roughly one percent. The reason for the loss of energy in excess of expectations is unknown.

The sound speed in bulk water is roughly 1480 m/s. Because of the high compressibility of water, little reduction in sound speed occurs as a result of the tube wall elasticity. The sound speeds for the three cases condensed in Chapter III are 1463 m/s, 1468 m/s and 1450 m/s, respectively. A description of each case in water is given in Appendix I, and the time of flight results for each case are given in Appendix J. The time of flight results are consistent with boundary condition (c).

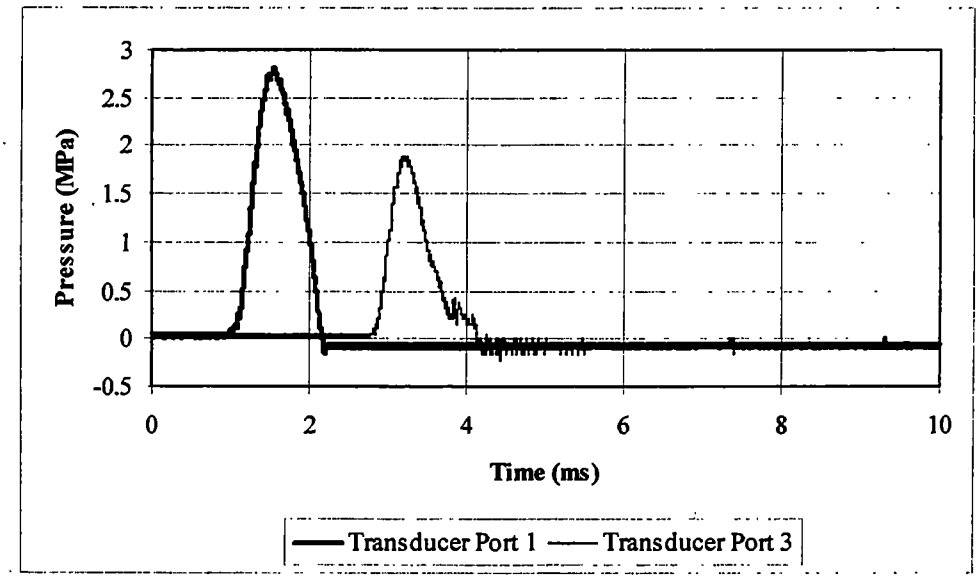


Figure 12 – Water Data Taken With Rubber Impact Diaphragm, 0.020-Inch Stainless Steel Coupon, No Flow In Waveguide, Transducer 1 In Port P1, Transducer 2 In Port P3

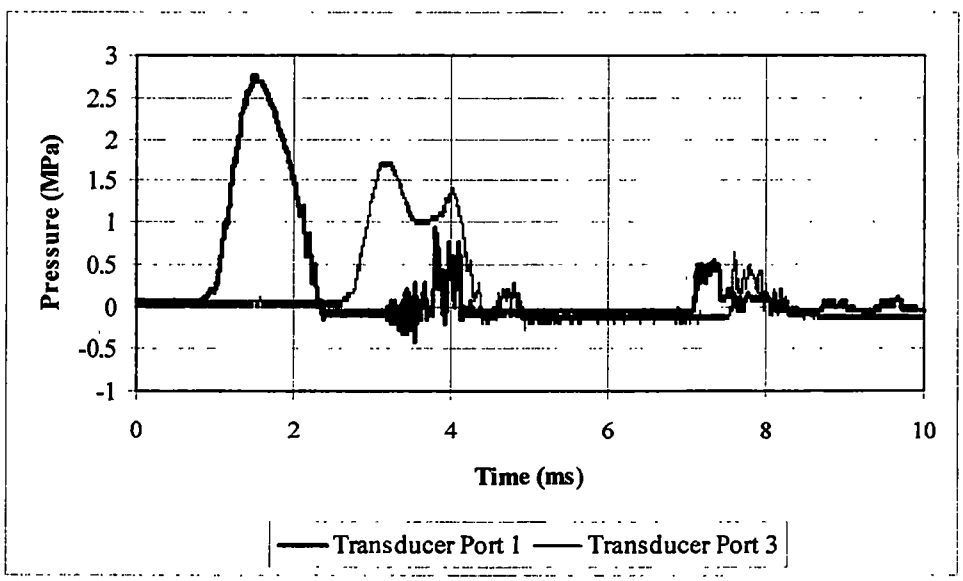


Figure 13 – Water Data Taken With Rubber Impact Diaphragm, 0.020-Inch Stainless Steel Coupon, 83 kPa (12 Psid) Across Waveguide, Transducer 1 In Port P1, Transducer 2 In Port P3

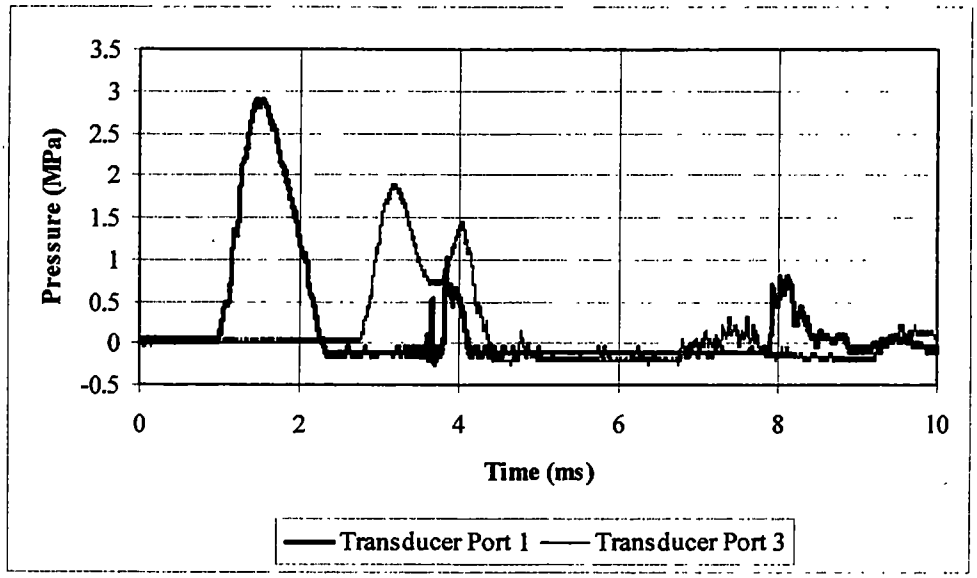


Figure 14 – Water Data Taken With Rubber Impact Diaphragm, 0.020-Inch Stainless Steel Coupon, 255 kPa (37 Psid) Across Waveguide, Transducer 1 In Port P1, Transducer 2 In Port P3

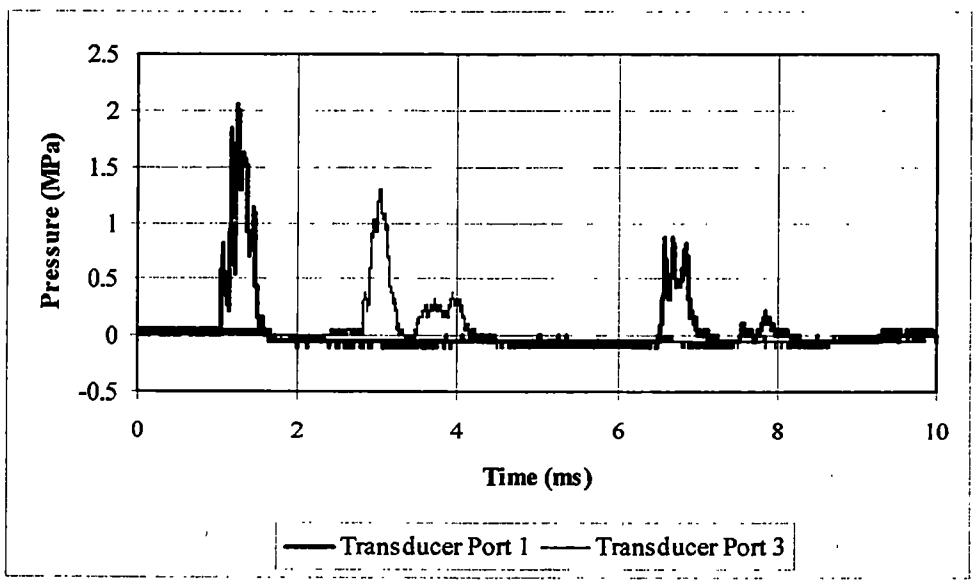


Figure 15 – Water Data Taken With 0.063-Inch Stainless Steel Impact Diaphragm, 0.025-Inch Stainless Steel Coupon, No Flow In Waveguide, Transducer 1 In Port P1, Transducer 2 In Port P3

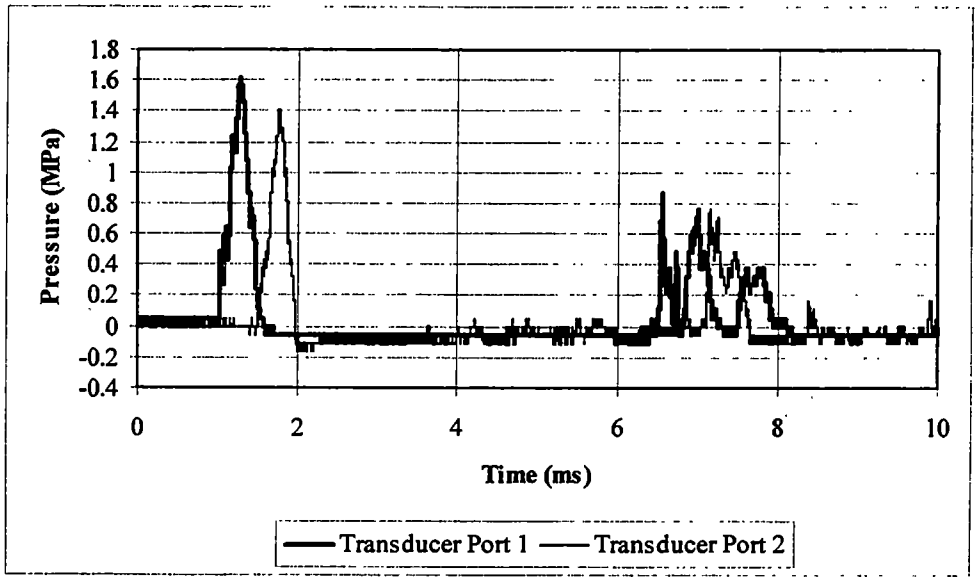


Figure 16 – Water Data Taken With 0.063-Inch Stainless Steel Impact Diaphragm, 0.025-Inch Stainless Steel Coupon, No Flow In Waveguide, Transducer 1 In Port P1, Transducer 2 In Port P2

CHAPTER VI

RESULTS IN MERCURY

Figure 17 and 18 represent data taken with mercury in the waveguide. A 0.010-inch stainless steel reflection coupon was used. There was no flow in the waveguide. The reflection diaphragms employed were 0.025-inch stainless steel and 0.010-inch stainless steel, respectively.

A description of each case is located in Appendix I. The time of flight results for each case are located in Appendix J. The time of flight results are most consistent with boundary condition (c), considered in Chapter III.

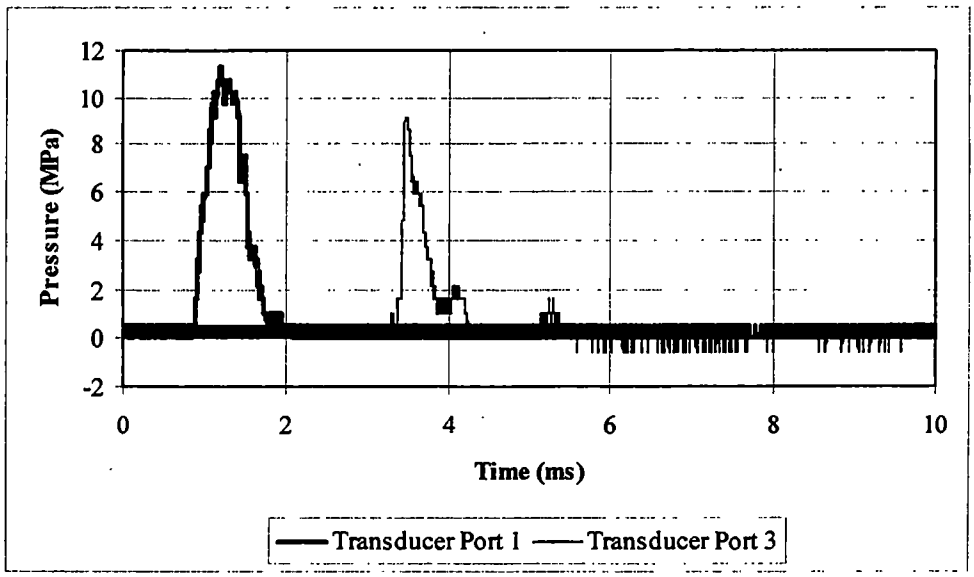


Figure 17 – Mercury Data Taken With 0.025-Inch Stainless Steel Impact Diaphragm, 0.010-Inch Stainless Steel Coupon, No Flow In Waveguide, Transducer 1 In Port P1, Transducer 2 In Port P3

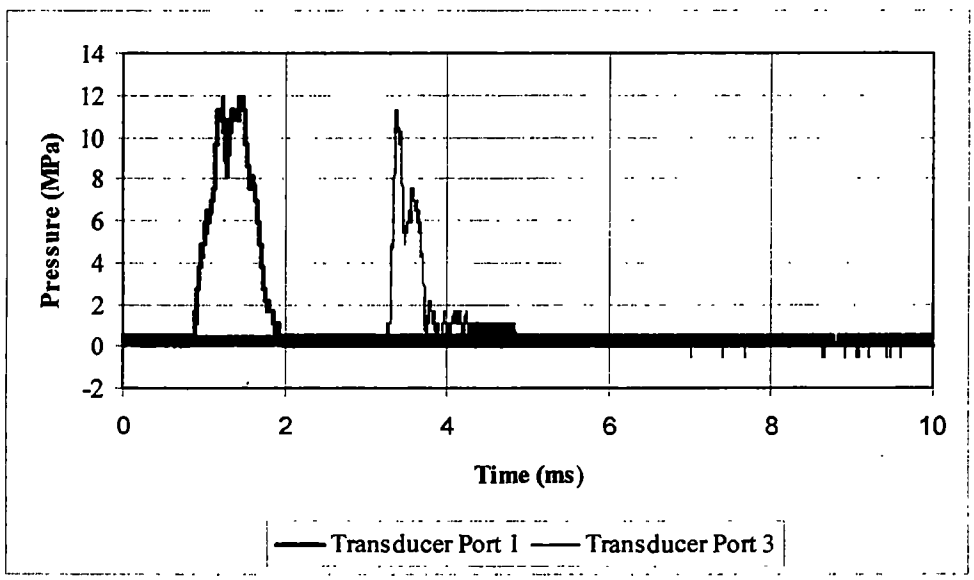


Figure 18 – Mercury Data Taken With 0.010-Inch Stainless Steel Impact Diaphragm, 0.010-Inch Stainless Steel Coupon, No Flow In Waveguide, Transducer 1 In Port P1, Transducer 2 In Port P3

CHAPTER VII

CONCLUSIONS

The experimental facility permits the collection of data that characterize the interaction of large amplitude pressure waves with various structures. Incident pressure waves exceeding 6.89 MPa (1000 psi) are possible in mercury with pulse widths less than one millisecond. Various materials are used to reflect these waves, and the effect of material properties and surface condition can be examined by observing variations in incident and reflected pressure waves. Preliminary data indicate that the waveguide has losses into branches in excess of that anticipated by design analysis. However, this does not affect the utility of the facility significantly since pressure measurements at transducer location P3 can be made without branches between the incident wave and reflecting coupon. The facility provides data suitable for validation of the material physics codes used to simulate the SNS target response to the proton pulse deposition.

CHAPTER VIII

FUTURE WORK

Several recommended changes could improve the usefulness of the waveguide. Presently, the waveguide has two pressure transducers and three pressure transducer ports. Most data are taken with transducers in ports 1 and 3. If additional data is desired from transducer port 2, the waveguide must be drained, and the transducer in port 3 must be moved to port 2. Then the waveguide is evacuated and filled. The movement of the transducer is an opportunity for mercury leaks and for damage to the instrument. The first recommendation is that a third transducer be acquired to avoid these risks. Instrumentation additional to a third transducer would also be helpful to the code validation mission for the facility. The back side of the reflection coupons is accessible. The second recommendation is that an accelerometer or high frequency proximity probe be acquired to study the deflection of these coupons when the pressure waves arrive. Also, a high frequency pressure transducer or accelerometer may be able to detect the noise commonly associated with cavitation at the mercury-coupon interface. This would supplement any evidence of cavitation observed in reflected pressure waves.

The data acquisition system consists of a 80486 computer and an AT-5102 digital oscilloscope card. The AT-5102 is a two channel device. If additional instrumentation is installed, it is important that data be collected from all instruments simultaneously. This permits a better comparison of physical information associated with the response. The third recommendation is that a data acquisition card be purchased that is capable of collecting data on more than two channels.

The current pulse is longer that the transit time from measurement location 3 to the reflection coupon and back to measurement location 3. Therefore, the reflected and incident waves overlap. A shorter pressure pulse width would allow easier data reduction and interpretation. The fourth recommendation is that a less compliant piston tip be added. This will shorten the impact time and, consequently, the pulse width. The fifth recommendation is that a less massive piston be added. This will also shorten the impact time and pulse width.

REFERENCES

Idelchik, I. E. 1994. *Handbook of Hydraulic Resistance*, 3d ed. Ann Arbor: CRC Press.

Kinsler, Lawrence, and Frey, Austin. 1962. *Fundamentals of Acoustics*, 2d ed.. New York: John Wiley & Sons.

McGlaum, J. M., and Thompson, S. L. 1990 CTH: a three-dimensional shock-wave physics code. *International Journal of Impact Engineering* 10: 251-360.

Moody, F. F. 1944. Friction Factors for Pipe Flow. *Trans. ASME* 66: 671.

Nayyar, Mohinder L., ed. 1992. *Piping Handbook.* New York: McGraw Hill, Inc.

Norton, M. P. 1989. *Fundamentals of Noise and Vibration Analysis for Engineers.* New York: Cambridge University Press.

Oak Ridge National Laboratory. National Spallation Neutron Source Conceptual Design Report, Volume 1, The NSNS Collaboration. May 1997. NSNS/CDR-2/V1, http://www.ornl.gov/nsns/CDRDocuments/CDRSections/CDRSections.htm.

Parmakian, John. 1963. *Waterhammer Analysis.* New York: Dover Publications, Inc.

PCB Piezotronics, Inc. 3425-T Walden Ave, Depew, New York 14043-2417.

Scarton, H. A., and Rouleau, W. T. 1973. Axisymmetric waves in compressible Newtonian liquids contained in rigid tubes: steady-periodic mode shapes and dispersion by the method of eigenvalleys. *Journal of Fluid Mechanics* 58: 595-621.

APPENDICES

APPENDIX A

DERIVATION OF MECHANICAL WORK FROM EXPANSION OF AFFECTED VOLUME

The motivation for the pressure waves in the mercury target are examined to the first order herein to provide a basic understanding of why the pressure wave propagation in the target and associated fluid-structure interactions are important.

Work is Defined as

$$W = \int P dV, \qquad \text{[A-1]}$$

where volume and density are related by

$$V = \frac{m}{\rho}. \qquad \text{[A-2]}$$

Taking the first derivative of [A-2], assuming constant mass, m, yields

$$dV = -m\frac{d\rho}{\rho^2}. \qquad \text{[A-3]}$$

Substituting [A-3] into [A-1] gives

$$W = \int -mP\frac{d\rho}{\rho^2}. \qquad \text{[A-4]}$$

Recall that the definition of sound speed from thermodynamics is

$$c^2 = \frac{dP}{d\rho}, \qquad \text{[A-5]}$$

where the process line for the application of the derivative is yet to be established. In this case, pressure is a function of temperature and density,

$$P = P(\rho, T). \qquad \text{[A-6]}$$

Because pressure is a function of both temperature and density, its derivative is

$$dP = \frac{\partial P}{\partial \rho}d\rho + \frac{\partial P}{\partial T}dT. \qquad \text{[A-7]}$$

For a constant volume or density heat-up, the derivative becomes

$$dP = \frac{\partial P}{\partial T} dT . \qquad \text{[A-8]}$$

Hence, the sound speed equation can be rewritten as

$$c^2 = \frac{dP}{dT}\frac{dT}{d\rho}. \qquad \text{[A-9]}$$

The process line for the derivative in [A-5] is isentropic. However, the compressibility of a liquid is insensitive to the process line. Hence, [A-9] is permissible. [A-9] is rewritten, using [A-3], as

$$c^2 = -\frac{V^2}{m}\frac{dP}{dT}\frac{dT}{dV}. \qquad \text{[A-10]}$$

Solving in favor of dV gives

$$dV = -\frac{V^2}{mc^2}\frac{dP}{dT}dT, \qquad \text{[A-11]}$$

which is simplified to form

$$dV = -\frac{V^2}{mc^2}dP . \qquad \text{[A-12]}$$

Substitution of [A-11] into [A-1] yields

$$W = \int -\frac{V^2}{mc^2} PdP . \qquad \text{[A-13]}$$

Because volume is a function of pressure in a liquid but is only a slight function of pressure, it can be assumed it to be constant,

$$W = -\frac{V^2}{mc^2}\int PdP, \qquad \text{[A-14]}$$

when the range of integration is defined from $P = 0$ to $P = \delta P$. [A-14] can be rewritten to form

$$W = -\frac{V^2}{2mc^2}\delta P^2 . \qquad \text{[A-15]}$$

Replacing dp in [A-9] with a finite pressure change, δp, yields

$$\delta P = c^2 \delta T \frac{d\rho}{dT}, \qquad \text{[A-16]}$$

which can be substituted into [A-15] to form

$$W = -\frac{V^2 c^2}{2m}\left(\delta T \frac{d\rho}{dT}\right)^2 . \qquad \text{[A-17]}$$

Recall from thermodynamics that

$$Q = mc_v \delta T . \qquad \text{[A-18]}$$

[A-18] is substituted into [A-17] to obtain

$$W = -\frac{V^2 c^2}{2m}\left(\frac{Q}{mc_v}\frac{d\rho}{dT}\right)^2, \qquad \text{[A-19]}$$

which simplifies to

$$W = -\frac{1}{2m}\left(\frac{VcQ}{mc_v}\frac{d\rho}{dT}\right)^2 . \qquad \text{[A-20]}$$

[A-20] represents the work done on the target by an individual pressure pulse. Figure A-1 shows the work performed on the target as a function of target volume for one proton pulse, given an average energy deposition rate of one megawatt.

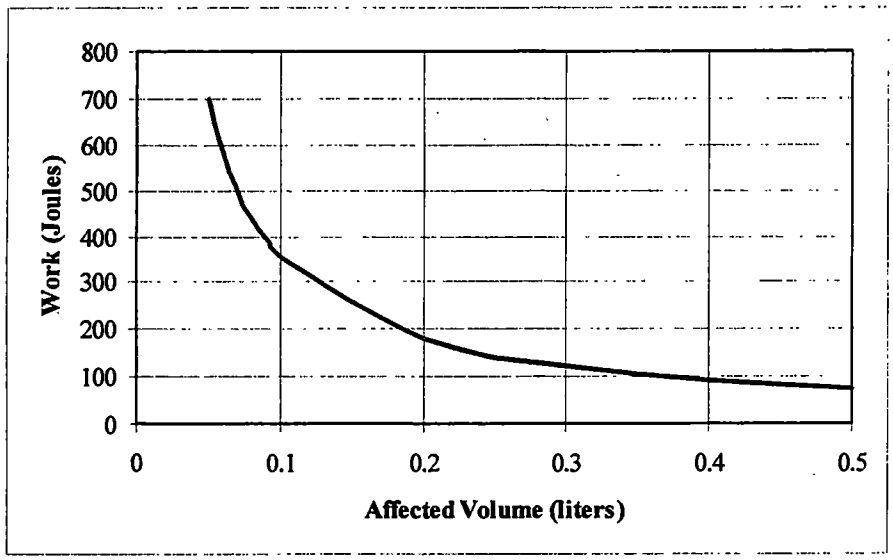


Figure A-1 – Work Performed On The Target As A Result Of One Proton Pulse Given An Average Energy Deposition Rate Of One Megawatt

APPENDIX B

DERIVATION OF SOUND SPEED AS A FUNCTION OF THE RATIO OF PIPING INNER DIAMETER TO WALL THICKNESS

In his book *Waterhammer Analysis*, John Parmakian performs a derivation for the effect of pipe wall elasticity on the sound speed of a fluid within a pipe (Parmakian 1963, 10-15). This derivation assumes that the wall of the pipe was thin with respect to the diameter of the pipe. The derivation given here considers situations where the wall thickness is significant with respect to the diameter. Additionally, Parmakian initiates system pressure perturbations by use of a column of water, $\rho g dH$, where ρ is the density of the fluid, g is gravitational acceleration, and dH is a change in the height of a column of the fluid. Here, a pressure perturbation dP is used.

Figure B-1 displays a moving control volume where velocity is a function of space and time:

$$v = v(x,t). \qquad \text{[B-1]}$$

The average velocity of the element face B as it is moving to plane D over time dt is

$$v + \frac{1}{2}\frac{\partial v}{\partial x}BD + \frac{1}{2}\frac{\partial v}{\partial t}dt, \qquad \text{[B-2]}$$

and the distance moved by face B during the time interval dt is

$$BD = \left(v + \frac{1}{2}\frac{\partial v}{\partial x}BD + \frac{1}{2}\frac{\partial v}{\partial t}\right)dt. \qquad \text{[B-3]}$$

Likewise, the distance moved by face C during the time interval dt is

$$CF = \left[v + \frac{\partial v}{\partial x}dx + \frac{1}{2}\frac{\partial}{\partial x}\left(v + \frac{\partial v}{\partial x}dx\right)CF + \frac{1}{2}\frac{\partial}{\partial t}\left(v + \frac{\partial v}{\partial x}dx\right)dt\right]dt. \qquad \text{[B-4]}$$

The change in length of element dx as the element moves from BC to DF is $BC - DF$. Neglecting higher order terms,

$$BD - CF = -\frac{\partial v}{\partial x}dxdt. \qquad \text{[B-5]}$$

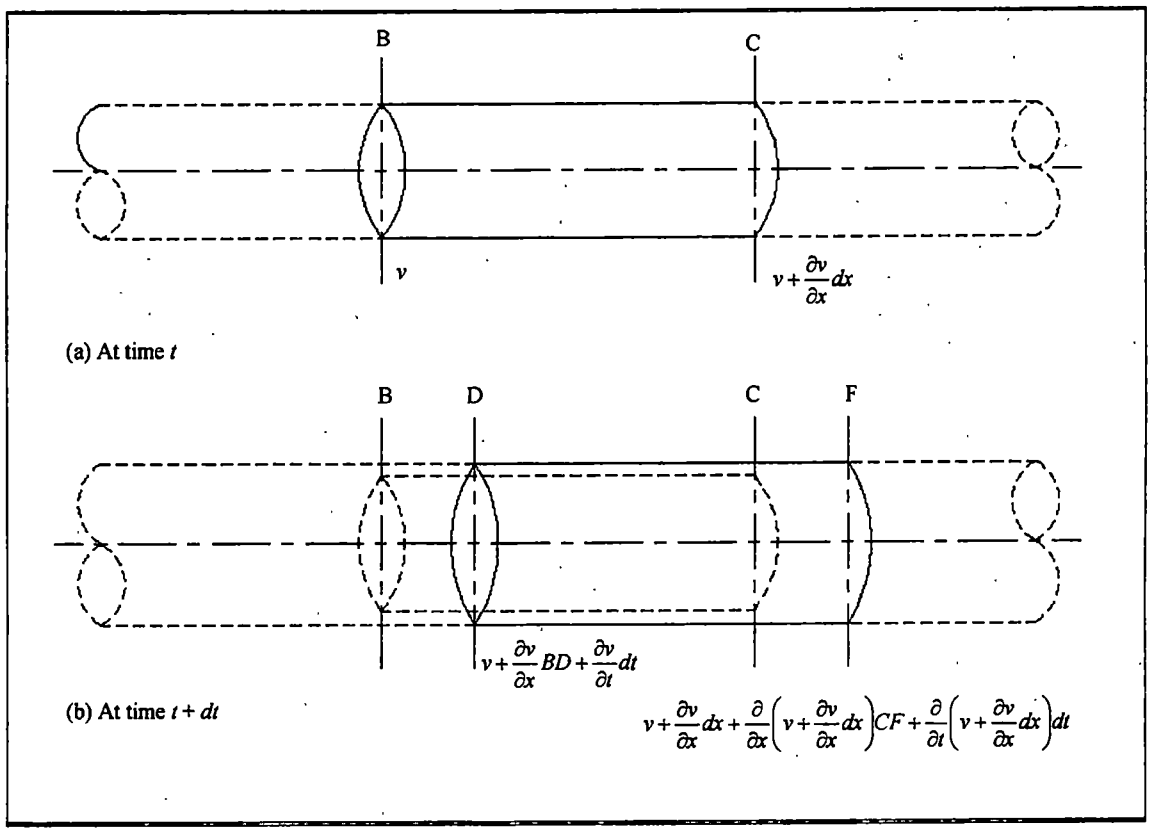


Figure B-1 - Diagram Of The Control Volume At Time T And At Time $T + Dt$ (Parmakian 1962, 11).

One factor influencing the change in length of element dx is the elasticity of the pipe wall, which causes it to expand or contract as pressure changes. This changes the cross-sectional area, changing the length of the volume element, which maintains a constant volume. The deformation of the inner radius of an element of the pipe shell produced by a change in longitudinal and circumferential stress is

$$\Delta R = \frac{R+\frac{e}{2}}{E}\left(\Delta\sigma_2 - \mu\Delta\sigma_1\right), \qquad \text{[B-6]}$$

where e is the wall thickness of the pipe and where $\Delta\sigma_1$ and $\Delta\sigma_2$ are the changes in the longitudinal and circumferential stresses, respectively, that result from a change in the fluid pressure. The change in the axial length of the element is

$$\delta x = \frac{dx}{E}(\Delta\sigma_1 - \mu\Delta\sigma_2). \qquad \text{[B-7]}$$

[B-6] can be rearranged to form

$$\frac{2\Delta R}{R}dx = \frac{2\frac{R+\frac{e}{2}}{E}(\Delta\sigma_2 - \mu\Delta\sigma_1)}{R}dx = \left(\frac{2}{E} + \frac{e}{ER}\right)(\Delta\sigma_2 - \mu\Delta\sigma_1)dx. \qquad \text{[B-8]}$$

[B-7] and [B-8] are combined to form

$$\delta x + \frac{2\Delta R}{R}dx = \frac{dx}{E}(\Delta\sigma_1 - \mu\Delta\sigma_2) + \frac{dx}{E}(\Delta\sigma_2 - \mu\Delta\sigma_1). \qquad \text{[B-9]}$$

This system is solved for the different cases of pipe wall boundary conditions described in Chapter III.

Case (a), a pipe anchored at the left end, free to move in a longitudinal direction throughout its length, and without expansion joints, is derived below. The principal stresses $\Delta\sigma_1$ and $\Delta\sigma_2$ can be expressed as

$$\Delta\sigma_1 = \frac{Ddp}{4e} \qquad \text{[B-10]}$$

and

$$\Delta\sigma_2 = \frac{Ddp}{2e}, \qquad \text{[B-11]}$$

where, D is the inner diameter of the pipe. Subsitution of [B-10] and [B-11] into [B-9] yields

$$\delta x + \frac{2\Delta R}{R}dx = \frac{dx}{E}\left(\frac{Ddp}{4e} - \frac{\mu Ddp}{2e}\right) + \frac{dx}{E}\left(2 + \frac{e}{R}\right)\left(\frac{Ddp}{2e} - \frac{\mu Ddp}{4e}\right), \qquad \text{[B-12]}$$

which is simplified to form

$$\delta x + \frac{2\Delta R}{R} dx = \frac{Ddpdx}{Ee} c_1, \qquad \text{[B-13]}$$

where

$$c_1 = \left(\frac{1}{4} - \frac{\mu}{2}\right) + \left(2 + \frac{e}{R}\right)\left(\frac{1}{2} - \frac{\mu}{4}\right). \qquad \text{[B-14]}$$

Case (b), a pipe anchored against longitudinal movement throughout its length, is derived below. The principal stresses $\Delta\sigma_1$ and $\Delta\sigma_2$ are defined as

$$\Delta\sigma_1 = \frac{\mu Ddp}{2e} \qquad \text{[B-15]}$$

and

$$\Delta\sigma_2 = \frac{Ddp}{2e}. \qquad \text{[B-16]}$$

Substitution of [B-15] and [B-16] into [B-9] yields

$$\delta x + \frac{2\Delta R}{R} dx = \frac{dx}{E}\left(\frac{\mu Ddp}{2e} - \frac{\mu Ddp}{2e}\right) + \frac{dx}{E}\left(2 + \frac{e}{R}\right)\left(\frac{Ddp}{2e} - \frac{\mu^2 Ddp}{2e}\right), \qquad \text{[B-17]}$$

which is simplified to form

$$\delta x + \frac{2\Delta R}{R} dx = \frac{Ddpdx}{Ee} c_1, \qquad \text{[B-18]}$$

where

$$c_1 = \left(1 + \frac{e}{2R}\right)\left(1 - \mu^2\right). \qquad \text{[B-19]}$$

Case (c), a pipe which has expansion joints between anchors throughout the length of the pipe, is derived below. The principle stresses $\Delta\sigma_1$ and $\Delta\sigma_2$ are

$$\Delta\sigma_1 = 0 \qquad \text{[B-20]}$$

and

$$\Delta\sigma_2 = \frac{Ddp}{2e}. \qquad \text{[B-21]}$$

Substitution of [B-20] and [B-21] into [B-9] yields

$$\delta x + \frac{2\Delta R}{R}dx = \frac{dx}{E}\left(0 - \frac{\mu Ddp}{2e}\right) + \frac{dx}{E}\left(2 + \frac{e}{R}\right)\left(\frac{Ddp}{2e} - 0\right), \qquad \text{[B-22]}$$

which can be simplified to form

$$\delta x + \frac{2\Delta R}{R}dx = \frac{Ddpdx}{Ee}c_1, \qquad \text{[B-23]}$$

where

$$c_1 = \left(2 + \frac{e}{R}\right) - \frac{\mu}{2}. \qquad \text{[B-24]}$$

In addition, the fluid has its own elasticity, which causes a volume change dV under the influence of a change in pressure dp,

$$dV = \frac{\pi R^2}{B_T}dpdx. \qquad \text{[B-25]}$$

This volume change causes the length of the fluid element to change, which becomes

$$\frac{\pi R^2}{B_T \pi R^2}dpdx = \frac{1}{B_T}dpdx. \qquad \text{[B-26]}$$

Therefore, the total change in length of the volume element as a result of a pressure change dp, taking into account both the compressibility of the fluid and the elasticity of the pipe wall is

$$BD - CF = \left(\frac{1}{B_T} + \frac{Dc_1}{Ee}\right)dpdx. \qquad \text{[B-27]}$$

System pressure is a function of space and time,

$$p = p(x,t). \qquad \text{[B-28]}$$

Also, fluid velocity is defined as

$$\frac{dx}{dt} = v. \qquad \text{[B-29]}$$

Taking the derivative of pressure, p, yields

$$dp = \frac{\partial p}{\partial t}dt + \frac{\partial p}{\partial x}dx = \frac{\partial p}{\partial t}dt + \frac{\partial p}{\partial x}\frac{dx}{dt}dt = \left(\frac{\partial p}{\partial t} + v\frac{\partial p}{\partial x}\right)dt. \qquad \text{[B-30]}$$

Substitution of [B-30] into [B-27] gives

$$BD - CF = \left(\frac{1}{B_T} + \frac{Dc_1}{Ee}\right)\left(\frac{\partial p}{\partial t} + v\frac{\partial p}{\partial x}\right)dxdt. \qquad \text{[B-31]}$$

Substitution of [B-5] into [B-31] yields

$$-\frac{\partial v}{\partial x} = \left(\frac{1}{B_T} + \frac{Dc_1}{Ee}\right)\left(\frac{\partial p}{\partial t} + v\frac{\partial p}{\partial x}\right), \qquad \text{[B-32]}$$

which can be rearranged to form

$$\frac{\partial p}{\partial t} + v\frac{\partial p}{\partial x} = -\frac{1}{\left(\frac{1}{B_T} + \frac{Dc_1}{Ee}\right)}\frac{\partial v}{\partial x}. \qquad \text{[B-33]}$$

Recall that

$$dp = \rho g dH. \qquad \text{[B-34]}$$

Substitution of [B-34] into [B-33] yields one of the fundamental water hammer equations (Parmakian 1963, 14-15),

$$\frac{\partial H}{\partial t} + v\frac{\partial H}{\partial x} = -\frac{c^2}{g}\frac{\partial v}{\partial x}, \qquad \text{[B-35]}$$

where

$$c = \sqrt{\frac{1}{\rho\left(\frac{1}{B_T} + \frac{Dc_1}{Ee}\right)}}. \qquad \text{[B-36]}$$

In [36], c is the sound speed of the fluid in the system, and there are three different cases of c_1:

$$\text{(a) } c_1 = \left(\frac{1}{4} - \frac{\mu}{2}\right) + \left(2 + \frac{e}{R}\right)\left(\frac{1}{2} - \frac{\mu}{4}\right) \qquad \text{[B-37]}$$

$$\text{(b) } c_1 = \left(1 + \frac{e}{2R}\right)\left(1 - \mu^2\right) \qquad \text{[B-38]}$$

$$\text{(c) } c_1 = \left(2 + \frac{e}{R}\right) - \frac{\mu}{2}. \qquad \text{[B-39]}$$

The sound speeds in mercury in the waveguide for the three cases are shown in Figure B-2.

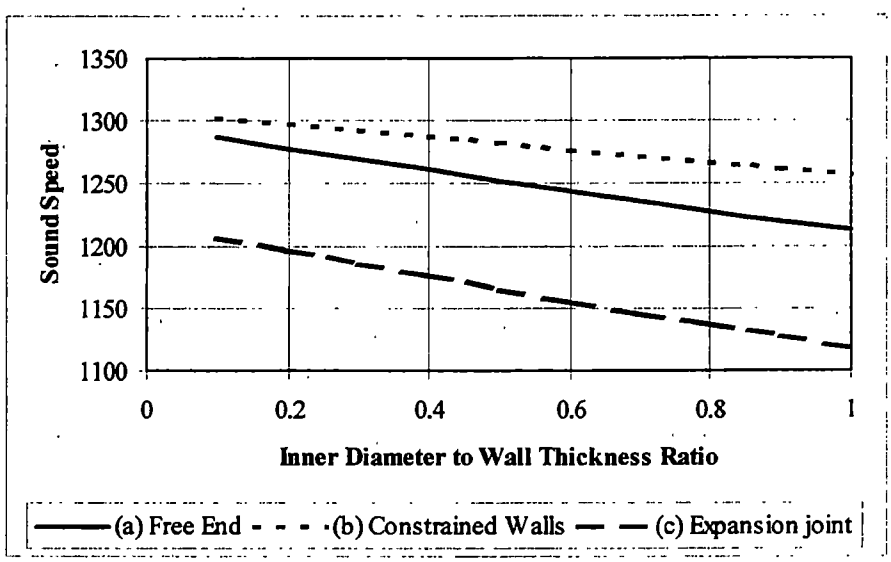


Figure B-2 – Sound Speed In Mercury In The Waveguide

APPENDIX C

PRESSURE DROP CALCULATIONS

The sponsor required flow in the waveguide with velocities up to 1 m/s. The design of the facility therefore required evaluation of pressure losses in the waveguide and fittings in order to establish elevation changes and/or pump characteristics necessary to attain the desired flow.

The fundamental velocity analyzed is 1 m/s in the 1/4-inch waveguide section. From this velocity, the velocities in all other sections of tubing can be determined. This information can be used to calculate the pressure drop for the tubing of each size used by means of

$$\Delta P = \frac{1}{2}\rho v^2 f \frac{L}{D_h}. \qquad \text{[C-1]}$$

Table C-1 displays hydraulic diameter (D_h), length (L), flow velocity (v), Reynold's number (Re), friction factor (f), and pressure drop (ΔP) for each size of tubing in the system. Table C-1 only displays the pressure drop information in the tubing The friction factors were taken from a Moody diagram (Moody 1944).

In the system, there are three fundamental classes of fittings: reducers, valves and elbows. The reducers are broken into two sets: those involving a sudden decrease in cross-sectional area and those involving a sudden increase in cross-sectional area. Those generating a sudden decrease in cross-sectional area are modeled as follows:

$$C_f = 0.5\left(1 - \frac{S_0}{S_1}\right)^{\frac{3}{4}}, \qquad \text{[C-2]}$$

where C_f is the fitting pressure drop coefficient, corresponding to fL/D_h (Idelchik 1994, 197-8). S_0 is the downstream cross-sectional area, and S_1 is the upstream cross-sectional

area. For those generating a sudden increase in cross-sectional area, another equation is used:

$$C_f = \left(1 - \frac{S_0}{S_2}\right)^2, \qquad \text{[C-3]}$$

where S_0 is the upstream cross-sectional area and S_2 is the downstream cross-sectional area (Idelchik 1994, 208). The globe valves are assigned a C_f of 7.8 (Idelchik 1994, 550). The elbows represent the connection of a 0.1807-inch line into the side of a 0.75-inch line. Because no available models could be located, they were treated as a reducer and as an enlargement fitting, for friction coefficients of 0.48 and 0.89, respectively. Additionally, the head-tank-to-tubing connection has a C_f of 0.57 (Idelchik 1994, 160-1). The waveguide drain line outlet has a C_f of 1.0 (Idelchik 1994, 640). The table below displays the flow velocity in each fitting, assuming a 1 m/s flow velocity in the waveguide, the friction coefficient, C_f, for each fitting and the pressure drop for each fitting. The pressure drop for each fitting was calculated by means of the following equation:

$$\Delta P = \frac{1}{2}\rho v^2 C_f, \qquad \text{[C-4]}$$

where the velocity, v, is the inlet velocity of the fitting unless there is no inlet velocity, as in the head tank drain connection. In this case, the outlet velocity is used. Table C-2 provides the pressure drop information for the fittings in the waveguide piping system.

If the pressure drop of the fittings is added to that of the piping, the total pressure drop is 175.5 kPa. The available pressure drop to drive the flow of mercury through the waveguide is calculated as follows:

$$\Delta P = \rho g h, \qquad \text{[C-5]}$$

where the height, h, is 9 feet or 2.74 meters, and the density, ρ, is 13,600 kg/m^3 (Holman 1990, 664). The available pressure drop is 366 kPa. Although this is not an exact method, the pressure drop, ΔP, is roughly proportional to the square of the fluid velocity, v. Therefore, the following relationship exists:

$$\frac{\Delta P_1}{\Delta P_2} \cong \frac{v_1^2}{v_2^2}. \qquad \text{[C-6]}$$

This relationship can be used to obtain v_2:

$$v_2 = v_1 \sqrt{\frac{\Delta P_2}{\Delta P_1}}, \qquad \text{[C-7]}$$

where v_1 is 1 m/s, ΔP_1 is the pressure drop necessary to generate a velocity in the waveguide of 1 m/s, and ΔP_2 is the available pressure drop in the system. The velocity that can theoretically be achieved in the waveguide is 1.44 m/s. The actual flow rate in the system that can be obtained through gravity driven flow has never been measured using mercury. However, it has been measured using water. The maximum flow velocity of water in the waveguide that can be obtained by means of gravity driven flow is 0.8 m/s. The basic Bernoulli equation is

$$\Delta P = \frac{1}{2}\rho v^2 \left(f \frac{L}{D} + C_f \right). \qquad \text{[C-8]}$$

When the pressure drop ΔP across the system is the result of a column of fluid, the Bernoulli equation becomes

$$\rho g H = \frac{1}{2}\rho v^2 \left(f \frac{L}{D} + C_f \right), \qquad \text{[C-9]}$$

which simplifies to

$$gH = \frac{1}{2}v^2\left(f\frac{L}{D} + C_f\right). \qquad \text{[C-10]}$$

This indicates that any fluid, regardless of its density, should have the same flow velocity in the waveguide as another fluid when the flow is controlled by gravity. Hence, the mercury can be expected to have a maximum flow velocity of 0.8 m/s in the waveguide when the system flow is controlled by gravity. For higher flow velocities, a pump is required.

Table C-1 – Pressure Drop Information For The Tubing In The Waveguide System

Tubing Size	D_h (in.)	L (in.)	v (m/s)	Re	f	ΔP (kPa)
½ inch	0.5	95	0.25	2.79E4	0.023	1.9
¼ inch	0.25	142	1.0	5.57E4	0.02	77.2
0.1807 inch	0.1807	6	1.92	7.73E4	0.019	15.7
Total						94.8

Table C-2 – Pressure Drop Information For The Fittings In The Waveguide System

Fitting	Velocity (m/s)	C_f	ΔP (kPa)
Head Tank Drain	0.25	0.57	0.242
Inlet Valve	0.25	7.8	3.315
Reducer (0.5 to 0.1807 inch)	1.92	0.45	11.3
Connection (0.1807 to 0.75 inch)	1.92	0.89	22.3
Reducer (0.75 to 0.25 inch)	1.0	0.46	3.14
Enlargement (0.25 to 0.75 inch)	1.0	0.79	5.372
Connection (0.75 to 0.1807 inch)	1.92	0.48	12.0
Enlargement (0.1807 to 0.5 inch)	1.92	0.76	19.051
Outlet Valve	0.25	7.8	3.315
Tubing Outlet	0.25	1.0	0.425
Total			80.7

APPENDIX D

ACOUSTIC BOUNDARY ANALYSIS

A first order evaluation of the response of the reflection coupon to the incident pressure wave is given here. This evaluation is appropriate to low amplitude pressure waves and only incorporates linear models. The physics of the interaction described is instructive but may not be representative of the response to high amplitude pressure waves.

Acoustic theory holds that when an acoustic wave is incident upon an interface between two media, two waves are produced. These waves are a reflected wave and a transmitted wave. The phase of the reflected wave is a function of the acoustic impedances of the two materials. If the acoustic impedance of medium 1 is lower than that of medium 2, the reflected wave is in phase. If, however, the acoustic impedance of medium 1 is lower than that of medium 2, the reflected wave is out of phase.

The acoustic theory described above relies on a single assumption, that the thicknesses of the media are significantly greater than the wavelength of the incident acoustic wave. This is a very idealized condition. In real acoustic systems, the wavelength of an incident acoustic wave is greater than the thickness of the medium through which it travels. In this case, the medium moves with the wave. There are three cases that describe the response of the medium. The motion can be dominated by the mass of the medium, the stiffness of the medium or the damping of the system. When the frequency of the incident wave is less than the natural frequency of the plate, the stiffness dominates. When the frequency is roughly equal to the plate's fundamental frequency, the damping dominates. When the frequency is greater than the fundamental frequency, the mass dominates (Norton 1989, 209-10).

Figure D-1 represents an acoustic boundary that is in contact with two separate fluids. On the left is mercury, and on the right is air. An incident pressure wave is propagating through the mercury. Once it is transmitted through the boundary, its energy cannot be transmitted into the air because the air has a miniscule acoustic impedance. Instead, the acoustic energy is applied to the reflected wave. The effect of the two pressure waves on the boundary is to cause it to flex with the wave. From Figure D-1, it is obvious that the balance of forces on the boundary is

$$P_i - P_r = \frac{F}{S}. \qquad \text{[D-1]}$$

The forces applied to the boundary that are represented by the term F in [D-1] are associated with the acceleration, damping and spring stiffness of the boundary. As the boundary flexes with the incident pressure P_i and the reflected pressure P_r, it is

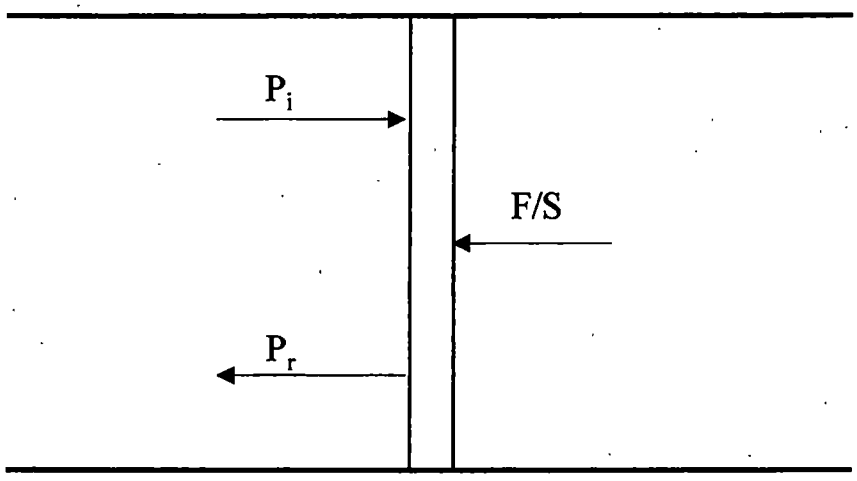


Figure D-1 – Diagram Of The Forces Associated With An Acoustic Boundary.

accelerated. The force F_a associated with this acceleration is

$$F_a = m\frac{\partial^2 \xi}{\partial t^2}, \qquad \text{[D-2]}$$

where ξ is the displacement of the acoustic boundary. Also, when the boundary moves, it has velocity, and the damping force F_d associated with that velocity

$$F_d = C\frac{\partial \xi}{\partial t}, \qquad \text{[D-3]}$$

where C is the coefficient of viscous damping for the boundary. Finally, as the boundary flexes with the pressures applied to it, it has position. The boundary behaves as a spring when it is flexed, and the force associated with its spring stiffness is

$$F_s = k\xi_s, \qquad \text{[D-4]}$$

where k_s is the stiffness coefficient of the boundary, assuming that the boundary behaves as a linear spring. The forces associated with the acoustic boundary can be summed as

$$F = F_a + F_d + F_s. \qquad \text{[D-5]}$$

Substitution of [D-2], [D-3] and [D-4] into [D-5] yields

$$F = m\frac{\partial^2 \xi}{\partial t^2} + C\frac{\partial \xi}{\partial t} + k\xi_s. \qquad \text{[D-6]}$$

When [D-6] is substituted into [D-1],

$$P_i - P_r = m\frac{\partial^2 \xi}{\partial t^2} + C\frac{\partial \xi}{\partial t} + k\xi_s \qquad \text{[D-7]}$$

is obtained. Assume that the incident pressure wave is a sine wave given by

$$P_i = A\sin(\omega t - kx), \qquad \text{[D-8]}$$

and that the reflected pressure wave is another sine wave given by

$$P_r = B\sin(\omega t - kx - \phi), \qquad \text{[D-9]}$$

where ϕ is the phase shift of the reflected wave. The classical assumption is that the fluid and the interface move together such that

$$\left[\frac{\partial \xi}{\partial x}\right]_{x=0} = -\frac{P_{\text{int erface}}}{\rho_0 c^2}. \qquad \text{[D-10]}$$

Because the incident and reflected waves must have the same energy in steady state,

$$A = B. \qquad \text{[D-11]}$$

Substituting [D-8] and [D-9] into [D-7], incorporating [D-11], yields

$$A[\sin(\omega t - kx) - \sin(\omega t - kx - \phi)] = m\frac{\partial^2 \xi}{\partial t^2} + C\frac{\partial \xi}{\partial t} + k\xi_s. \qquad \text{[D-12]}$$

[D-12] accounts for all possible influences on the motion of the acoustic boundary. When the system is stiffness dominated, [D-12] becomes

$$A[\sin(\omega t - kx) - \sin(\omega t - kx - \phi)] = k\xi_s. \qquad \text{[D-13]}$$

When the system is mass dominated, [D-12] becomes

$$A[\sin(\omega t - kx) - \sin(\omega t - kx - \phi)] = m\frac{\partial^2 \xi}{\partial t^2}. \qquad \text{[D-14]}$$

[D-12], [D-13] or [D-14] can be solved to determine the position, ξ, of the boundary and the phase shift, ϕ, of the reflected wave. If the phase shift is sufficiently high, the fluid is placed under tension and may cavitate.

APPENDIX E

BRANCH ANALYSIS

The waveguide has several branches and small cross-section variations to support venting operations, fluid flow and instrumentation. These influence the propagation of the pressure wave and are evaluated herein.

An acoustic branch can be categorized by the relative lengths of the branch and the wavelength of the acoustic field passing through the waveguide. If the wavelength is less than the length of the branch, the branch can be analyzed as a standard branch connection. Otherwise, the branch is considered a Helmholz oscillator, which is a resonator that serves as a mechanical filter.

Acoustic Branch (Kinsler and Frey 1962, 203-5)

Consider the branch connection shown in Figure E-1 below. There are four pressure waves under consideration. The incident pressure wave, p_i, gives rise to the transmitted wave, p_t, the reflected wave, p_r, and the branch wave, p_b:

$$p_i = A_1 e^{j(\omega t - kx)} \qquad \text{[E-1]}$$

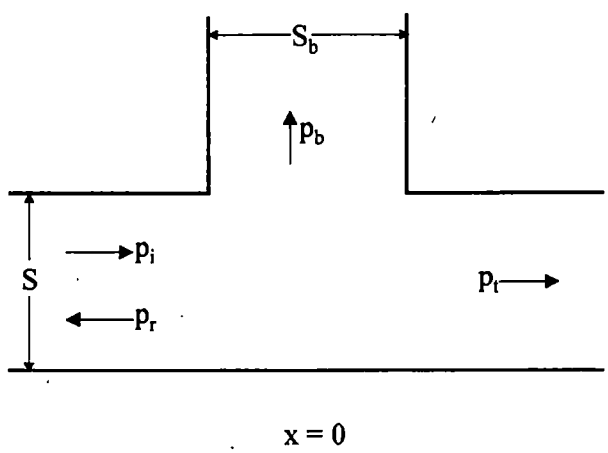


Figure E-1 – Diagram Of A Side Connection

$$p_t = A_2 e^{j(\omega t - kx)} \qquad \text{[E-2]}$$

$$p_r = B_1 e^{j(\omega t + kx)} \qquad \text{[E-3]}$$

and

$$p_b = A_b e^{j(\omega t - kx)}. \qquad \text{[E-4]}$$

With the assumption that the cross-sectional dimensions of the pipes are small with the wavelengths of the incident pressure wave, the relationship among the different pressures is

$$p_i + p_r = p_t = p_b. \qquad \text{[E-5]}$$

This can be solved to obtain:

$$\alpha_t = \frac{Z_b^2}{\left(\frac{\rho_0 c}{2S} + Z_b\right)^2} \qquad \text{[E-6]}$$

and

$$\alpha_r = \left(\frac{-\frac{\rho_0 c}{2S}}{\frac{\rho_0 c}{2S} + Z_b}\right)^2, \qquad \text{[E-7]}$$

where α_t and α_r are the transmission and reflection coefficients, respectively. The acoustic impedance of a transmitted wave, Z_t, is defined as

$$Z_t = \frac{\rho_0 c}{S}, \qquad \text{[E-8]}$$

where S is the cross-sectional area of the pipe. The branch impedance is

$$Z_b = \frac{S}{S_b}\frac{\rho_0 c}{S} = \frac{\rho_0 c}{S_b}, \qquad \text{[E-9]}$$

where S_b is the cross-sectional area of the branch. Substitution of [E-9] into [E-6] and [E-7] yields

$$\alpha_t = \left(\frac{2S}{2S + S_b} \right)^2 \qquad \text{[E-10]}$$

and

$$\alpha_r = \left(\frac{-2S_b}{2S + S_b} \right)^2 . \qquad \text{[E-11]}$$

By definition,

$$1 = \alpha_t + \alpha_r + \alpha_b \qquad \text{[E-12]}$$

such that the branch transmissivity coefficient can be determined from the transmissivity and reflectivity coefficients.

In the waveguide, there are five acoustic branches that are described in Table E-1. Of these branches, the impact end connections affect the pressure wave before it passes transducer 1. The vacuum pump suction line is between transducers 1 and 2, and it affects the pressure wave as it propagates between the two transducers. The reflection end connections affect the reflected pressure wave.

Helmholz Oscillators

The small fluid cavities formed at the instrumentation ports will act as Helmholz oscillators and limit the frequency response of the cavity and instrumentation assembly.

Consider the Helmholz oscillator shown in Figure E-2. It consists of a rigid enclosure with volume V that communicates with an external medium through an opening of radius a and length l. It behaves as a spring mass system in which the pressure of the fluid in the enclosure serves as the stiffness element, and the fluid in the opening serves

as the mass element. At the opening, the radiation of acoustic energy into the surrounding medium provides a resistance element. The fluid in the opening has an effective mass of $\rho_0 S_b l'$ where l' is the effective length of the opening. Some of the fluid beyond the opening moves with the fluid in the opening, increasing the effective mass. This effective length is modeled as

$$l' = l + 2\Delta l, \qquad \text{[E-13]}$$

where Δl, the end correction, can be modeled as

$$\Delta l = \frac{8a}{2\pi} \text{ (Kinsler and Frey 1962, 186-7).} \qquad \text{[E-14]}$$

The Helmholz oscillator has a double role as a mechanical filter. With respect to the acoustic energy passing from the medium to the volume element, the oscillator behaves as a low-pass filter whose upper frequency limit is its natural frequency. The pressure waves transmitted to the downstream side of the resonator experiences the effect of a band exclusion filter whose exclusion band is centered about the natural frequency of the oscillator. The natural frequency of a Helmholz resonator is

$$\omega_0 = c\sqrt{\frac{S_b}{l'V}} \text{ (Kinsler and Frey 1962, 193).} \qquad \text{[E-15]}$$

When a Helmholz oscillator is treated as a branch, the transmissivity, reflectivity and branch coefficients, respectively are

$$\alpha_t = \frac{R_b^2 + X_b^2}{\left(\frac{\rho_0 c}{2S} + R_b\right)^2 + X_b^2}, \qquad \text{[E-16]}$$

$$\alpha_r = \frac{\left(\frac{\rho_0 c}{2S}\right)^2}{\left(\frac{\rho_0 c}{2S} + R_b\right)^2 + X_b^2} \qquad \text{[E-17]}$$

and

$$\alpha_b = \frac{\frac{\rho_0 c}{2S} R_b}{\left(\frac{\rho_0 c}{2S} + R_b\right)^2 + X_b^2} \qquad \text{[E-18]}$$

(Kinsler and Frey 1962, 204-5).

If viscous losses are neglected, there is no net energy dissipation from the waveguide into the oscillator. Consequently,

$$R_b = 0. \qquad \text{[E-19]}$$

If the area of the resonator opening is

$$S_b = \pi a^2, \qquad \text{[E-20]}$$

the length of the neck is l, and the volume is V, then the acoustic reactance of the oscillator is

$$X_b = \rho_0 \left(\frac{\omega l'}{S_b} - \frac{c^2}{\omega V}\right). \qquad \text{[E-21]}$$

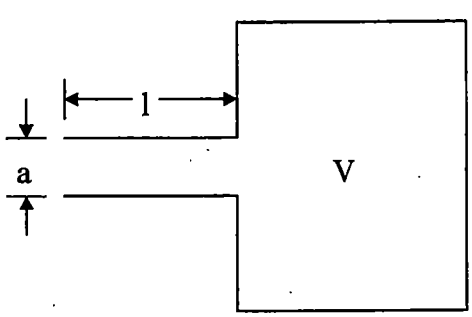


Figure E-2 – Diagram Of A Helmholz Resonator

$$X_b = \rho_0 \left(\frac{\omega l'}{S_b} - \frac{c^2}{\omega V} \right). \qquad \text{[E-21]}$$

Substitution of [E-21] into [E-16], [E-17] and [E-18] yields

$$\alpha_t = \frac{1}{1 + \frac{c^2}{4S^2 \left(\frac{\omega l'}{S_b} - \frac{c^2}{\omega V} \right)^2}}, \qquad \text{[E-22]}$$

$$\alpha_r = \frac{c^2}{1 + 4S^2 \left(\frac{\omega l'}{S_b} - \frac{c^2}{\omega V} \right)^2} \qquad \text{[E-23]}$$

and

$\alpha_b = 0$ (Kinsler and Frey 1962, 206). [E-24]

The transducer ports in the waveguide are identical Helmholz oscillators. In each one, the area of the opening, S_b, is $3.22*10^{-5}$ m^2. The length of the opening is $1.59*10^{-3}$ m. The effective length of the opening is theoretically 0.0054 m. The volume of the resonator is roughly $2.3*10^{-7}$ m^3. From these dimensions, the natural frequency of the oscillator is 34 kHz. The transmissivity and reflectivity of the transducer ports as a function of incident pressure wave frequency are shown in Figures E-3 and E-4.

Table E-1 – Acoustic Branches

Branch	S (m)	S_b (m)	α_t	α_r	α_b
Impact end vent	0.019	0.0046	0.80	0.012	0.19
Impact end drain	0.019	0.0046	0.80	0.012	0.19
Reflection end fill	0.019	0.0046	0.80	0.012	0.19
Reflection end drain	0.019	0.0046	0.80	0.012	0.19
Vacuum pump suction	0.0063	0.0016	0.80	0.049	0.15

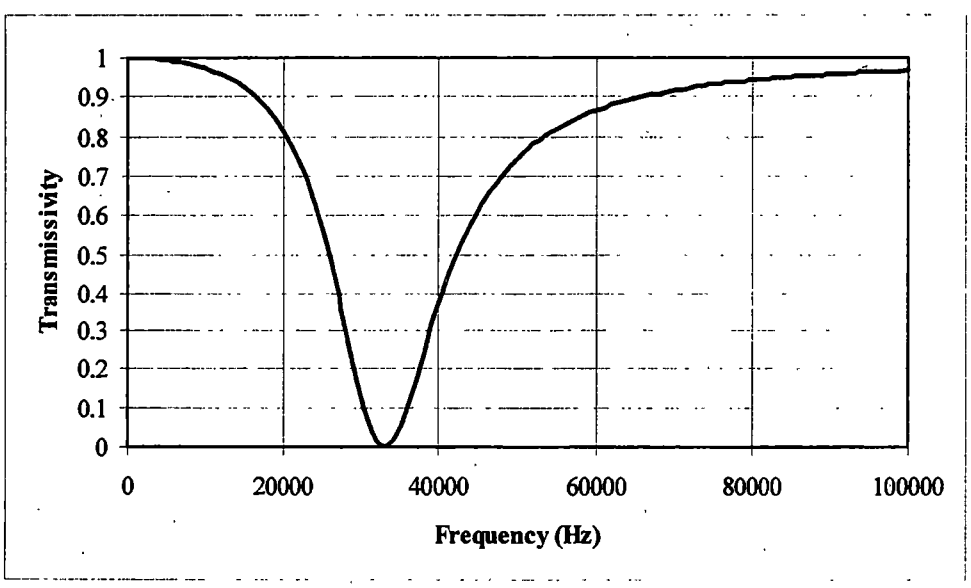


Figure E-3 – Transmissivity Of The Transducer Ports As A Function Of Incident Pressure Wave Frequency

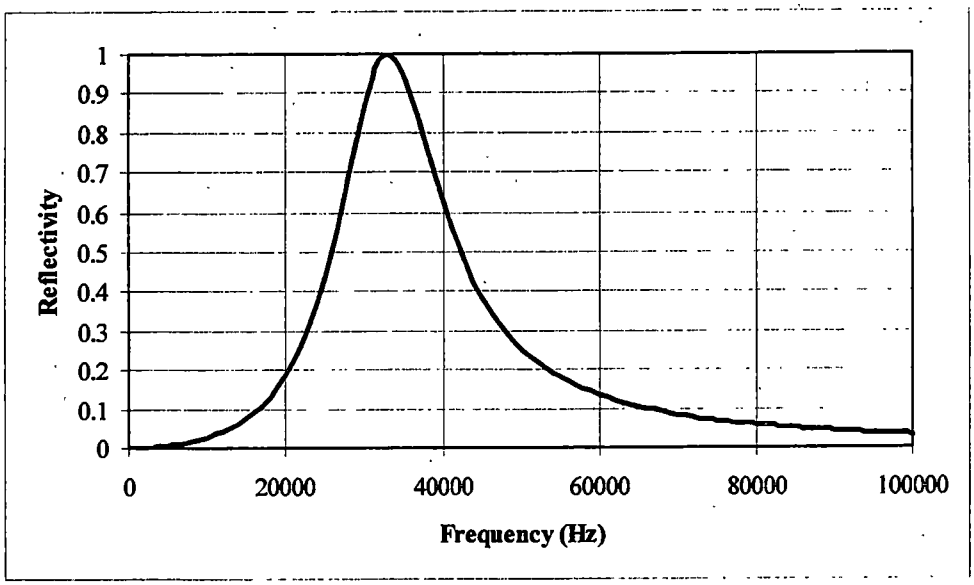


Figure E-4 – Reflectivity Of The Transducer Ports As A Function Of The Incident Pressure Wave Frequency

APPENDIX F

HYDRAULIC ACCUMULATOR SIZING CALCULATIONS

The mercury transfer pump is a positive displacement diaphragm pump. A diaphragm pump does not provide continuous discharge. Instead, its flow occurs in pulses, which cause pressure pulsations in the system. Because the waveguide is designed to study the effects of thermoacoustic pressure waves, it is not desired to complicate the pressure distribution within the waveguide. The pump is driven by an electric motor rotating at 1024 revolutions per minute. The motor is connected to the pump by a v-belt drive with a 3.5:1 turning ratio. Consequently, the pump rotates at 292.6 revolutions per minute. The time, τ, for one complete revolution is 0.206 second. However, the operation of the pump is such that first half of the stroke is used to pull mercury into the pump housing. The second half is used to push it out of the housing into the discharge piping. This operation is what causes the start-stop flow situation in the waveguide and consequent pressure pulsations. The discharge pulsation of the pump is a direct result of accelerating the fluid in the waveguide from a zero-flow condition to a maximum-velocity flow condition. Assuming a constant acceleration over the second half of the revolution, the volume, V, of mercury pumped in that time period and the maximum velocity, v_{max}, of the mercury can be related by

$$V = \frac{1}{2} v_{\max} \tau S . \qquad \text{[F-1]}$$

From the definition of acceleration,

$$a = \frac{dv}{dt}, \qquad \text{[F-2]}$$

it can be shown that

$$a = \frac{2 * v_{max}}{\tau}, \qquad \text{[F-3]}$$

assuming that the acceleration is constant. From [F-1] it can be determined that the maximum velocity is 40.5 m/s. This results in an acceleration of 393 m/s^2. The mass of the mercury in the waveguide is1.7 kg, and this is what must be accelerated to the maximum velocity. The pressure associated with that acceleration is

$$PS = ma. \qquad \text{[F-4]}$$

This pressure is 20.8 MPa, which is sufficient to interfere with the experimentation and is greater than the design discharge pressure of the pump of 1.4 MPa. The only way to avoid such high pressure oscillations in the system is to install a hydraulic accumulator in the system near the pump discharge.

A hydraulic accumulator consists of a gas bladder contained within a pressure vessel that is connected to the system. When the discharge pressure of the pump is high, it forces mercury into the accumulator, compressing the gas bladder adiabatically and dissipating the pressure pulsation of the acceleration of mercury out of the pump. When the discharge pressure of the pump falls, the pressure of the gas in the bladder expels the mercury from the accumulator, sustaining system pressure nearly constant. It is assumed that the action of the gas volume in the bladder is adiabatic, such that

$$\frac{P_2}{P_1} = \left(\frac{\upsilon_1}{\upsilon_2}\right)^{\gamma}, \qquad \text{[F-5]}$$

where υ is the specific volume of the gas, defined as

$$\upsilon = \frac{V_g}{m_g}. \qquad \text{[F-6]}$$

Let υ_1 be the volume of the gas in the accumulator when the bladder fills the volume of the accumulator, and let υ_2 be the volume of the gas in the accumulator when the mercury has been forced into the accumulator by pump discharge pressure. υ_1 and υ_2 are related by

$$\upsilon_2 = \upsilon_1 - \delta\upsilon, \qquad \text{[F-7]}$$

where $\delta\upsilon$ is the change in the specific volume of the gas that occurs when the volume of mercury enters the accumulator during the pump's discharge stroke. υ_1 and $\delta\upsilon$ are defined as

$$\upsilon_1 = \frac{V_g}{m_g} \qquad \text{[F-8]}$$

and

$$\delta\upsilon = \frac{\delta V}{m_g}, \qquad \text{[F-9]}$$

respectively, where δV is the volume of mercury that enters the accumulator during the pump's discharge stroke. Substitution of [F-7], [F-8] and [F-9] into [F-5] yields

$$\frac{P_2}{P_1} = \left(\frac{V_g}{V_g - \delta V}\right)^{\gamma}. \qquad \text{[F-10]}$$

It is desired that the nominal gas pressure, P_1, in the accumulator be 0.45 MPa (50 psig) and that the pressure oscillations be limited to 0.01 MPa. Hence, the maximum pressure in the accumulator, P_2, is 0.46 MPa. The transfer pump has a capacity of two gallons per minute, 7.57 liters per minute, or 25.9 cubic centimeters per revolution. It is not known how much of this volume actually enters accumulator, but the most conservative assumption is that all of it enters the accumulator. Air is to be used in the accumulator.

It has a ratio of specific heats, γ, of 1.4. It is determined that a minimum gas volume of 16.6 cubic centimeters is required. For a conservative design, a one-liter accumulator is used in the system.

APPENDIX G

PCB 102A04 PRESSURE TRANSDUCER SPECIFICATIONS

Dynamic Performance		
Dynamic Range (for ±V output)	psi (kPa)	1000 (6900)
Maximum Static Pressure	psi (kPa)	10000 (69000)
Resolution	psi (kPa)	0.02 (0.14)
Resonant Frequency	kHz	≥500
Rise Time (reflected)	µsec	≤1.0
Low Frequency Response (-5%)	Hz	0.005
Linearity	% FS	≤ 1
Environmental		
Acceleration Sensitivity	psi/g (kPa/m/s^2)	≤ 0.002 (≤ 0.0014)
Operating Temperature Range	°F (°C)	-100 to 275 (-73 to +135)
Temperature Coefficient of Sensitivity	%/°F (%/°C)	≤ 0.03 (≤ 0.054)
Maximum Flash Temperature	°F (°C)	3000 (5400)
Maximum Shock	g pk (m/s^2 pk)	20000 (196140)
Electrical		
Sensitivity	mV/psi (mV/kPa)	5 ± 0.3 (0.7 ± 0.04)
Output Polarity (positive pressure)		Positive
Discharge Time Constant (at room temp)	sec	≥100
Excitation Voltage Required	+ VDC	20 to 30
Excitation Constant Current Required	mA	2 to 20
Output Impedance	ohms	<100
Output Bias Voltage	+ VDC	9 to 14
Ground Isolation	ohms	10^8
Mechanical		
Structure	geometry	Compression
Sensing Element	material	Quartz
Case	material	Stainless Steel
Diaphragm	material	Invar
Sealing	type	Epoxy
Connector	type	10-32 Coaxial
Weight	oz (grams)	0.41 (11.6)

APPENDIX H

WAVEGUIDE EXPERIMENTAL DESIGN AND PLANNING REPORT

Waveguide Experimental Design and Planning Report

R. Harvill

September 11, 1998

Approvals:

Project Manager Rusi Taleyarkhan
Rusi Taleyarkhan

Safety: Richard Montgomery 9/11/98
Richard Montgomery

Quality Assurance: W. A. Miller
William Miller

OAK RIDGE NATIONAL LABORATORY
MANAGED BY LOCKHEED MARTIN ENERGY RESEARCH CORPORATION
FOR THE US DEPARTMENT OF ENERGY

POST OFFICE BOX 2009, Bldg. 9204-1
OAK RIDGE, TN 37831-8045

PHONE (423)-241-1715
FAX: (423) 574-0740
INTERNET: SRD@ornl.gov

Date: September 8, 1998

To: R. P. Taleyarkhan, R. Montgomery, R. Burnett, L. Hoch

From: R. Harvill

cc: W. G. Craddick, A. Ruggles

Subject: Revised wave guide experiment design and report

Attached is the revised wave guide experiment design and experiment report. It incorporates all suggestions made by R. Montgomery, B. Miller, R. Burnett, and L. Hoch, and is being routed (as requested by R. Montgomery) for formal signoff by the undersigned.

RPH:dmh

ornl - Bringing Science to Life

Waveguide Experimental Design and Planning Report
R. Harvill
September 1998

Waveguide Design

A waveguide/shock tube has been constructed to allow studies of pressure wave performance in mercury contained in stainless steel. The facility is shown in Figure 1 and consists of a waveguide with a diaphragm at one end that can be struck with a piston to create pressure pulses. The opposite end of the waveguide has a flange onto which material coupons can be attached. These coupons can have different structural and surface properties to establish the relationship between these properties and the pressure wave response. The waveguide is fitted with two pressure transducers.

A pressure pulse is formed within the waveguide when the piston is driven by spring force into the diaphragm at one end of the waveguide. This pressure pulse propagates down the waveguide and is detected and measured by the pressure transducers as it passes by their positions. When the pressure wave reaches the coupon at the opposite end of the waveguide, it reflects and propagates in the opposite direction down the waveguide. The nature of the reflection of the pressure pulse is determined by the material against which the pulse reflects. If the reflected pulse is out of phase with the incident pressure pulse, the mercury is placed under tension and may cavitate.

The system supporting the waveguide, shown in Figure 2, consists of two tanks and a transfer pump. This system has been designed to permit testing both when the mercury is stationary within the waveguide and when it is flowing through the waveguide. The head tank provides driving head for gravity induced flow through the waveguide, allowing tests under flowing conditions. The drain tank is used to collect the mercury when the waveguide is vented or drained and serves as the reservoir to which the mercury flows when testing is performed under flowing conditions. The mercury transfer pump is used to move mercury from the drain tank to the head tank. Because the mercury transfer pump is a positive displacement pump, its discharge is pulsed and causes pressure oscillations. Because these pressure perturbations would complicate pressure pulse studies in the waveguide, hydraulic accumulators have been installed on the suction and discharge of the pump to damp out these pressure perturbations. The flow in the waveguide is governed either by gravity or by the operation of the pump.

The waveguide is constructed from 3.7 meters of one-half-inch schedule xx stainless steel (316) tubing, which has an inner diameter of 0.0064 m and a wall thickness of 0.0075 m. The purpose of such thick-walled tubing is to provide a rigid boundary condition for waves passing through the waveguide. While the typical sound speed calculation for fluid in a pipe assumes a rigid boundary condition, real pipes are not perfectly rigid. Consequently, the flexibility of the pipe wall affects the sound speed in the combined fluid and pipe system. The theoretical sound speed in bulk mercury is roughly 1450 m/s. Calculations have been performed to determine the sound speed in the

waveguide filled with mercury when the pressure vessel walls are elastic and subject to the following boundary conditions:

(1) a tube fixed at one end, free to move longitudinally throughout its length and without expansion joints.
(2) a tube anchored against longitudinal movement throughout its length.
(3) a tube fixed at both ends with expansion joints throughout its length.

It should be noted that these calculations consider only the first mode of an infinite number of modes.

When the stainless steel pressure vessel is infinitely thick, the wall elasticity is minimal and the predicted sound speed is at a maximum. Table 1 shows the sound speed in mercury in an infinitely thick pressure vessel and for the mercury in the waveguide, which has an inner-diameter-to-wall-thickness ratio of 0.857, for the three boundary conditions previously described.

Table 1 – Waveguide sound speed as a function of boundary condition

Boundary Condition Case Number	Sound Speed	
	Infinitely thick walls	Waveguide
1	1296	1223
2	1307	1263
3	1218	1131

While all three cases are idealized conditions, the one most applicable to the waveguide is case two because the waveguide is restrained by shock mounts throughout its length. For this case, the sound speed for the waveguide is 1263 m/s representing a 3.4% reduction in sound speed. The 0.252-inch inner diameter of the waveguide minimizes the inventory of mercury in the waveguide. Because mercury is a hazardous material, it is desired to minimize its inventory at the test site. As a result of the small volume of the waveguide, $1.3*10^{-4}$ cubic meters, only 1.7 kilograms of mercury must be in the waveguide during testing. The small diameter permits temporal resolution of wavelengths down to five centimeters, corresponding to 23 kHz, for time of flight measurements and permits a plane wave assumption in the waveguide for these wavelengths. When a wave passes through small-diameter tubing, it causes fluid motion near the walls that can cause viscous dissipation of energy according to the following equation:

$$P = P_0 e^{-\alpha x} \tag{1}$$

where

$$\alpha = \frac{1}{ac}\sqrt{\frac{\eta\omega}{2\rho_0}} \tag{2}$$

For Equation (11), the shear coefficient of viscosity, η, is 0.0016 Ns/m^2, and the angular velocity, ω, is 15 kHz. The density, ρ, is 13, 600 kg/m^3. In the waveguide, this energy

dissipation amounts to roughly 7% for a wave travelling the 7.4 meters from the impact diaphragm to the reflection coupon and back to the impact diaphragm.

The 3.7-meter length of the waveguide permits reasonable temporal resolution of long wavelengths. The distance between transducers is roughly 2.5 meters, permitting resolution for frequencies as low as 505 Hz. The distance between transducer 2 and the reflection assembly is roughly one meter. Therefore a wavelength of 2 meters, corresponding to a frequency of 631 Hz, can be resolved without interference of both the incident and reflected wave at the transducer.

The waveguide reflection assembly consists of a blind flange with a 1.9-cm hole drilled through it. This permits the placement of coupons of different materials or different thicknesses of the same material at the end of the waveguide where the waves reflect. This permits the study of the effect of material composition or thickness on the mode of reflection of a wave. The compliance of the material determines the phase of the reflected wave with respect to the incident wave.

A solenoid is used to hold the piston that forms the pressure pulse in the waveguide. When current is initiated to the solenoid, the piston retracts into the solenoid. When the current is interrupted, a spring drives the plunger into the diaphragm at the end of the waveguide. As the diaphragm is pushed forward, it displaces a volume of fluid, initiating the pressure wave. The plunger has a teflon tip designed to distribute the impact forces evenly over the surface of the diaphragm. This arrangement is designed to produce a well-defined shock wave.

The pressure waves in the waveguide are detected and measured by means of two PCB 102A04 piezoelectric transducers. Each transducer has a frequency response of greater than 500 kHz and is designed for shock wave detection. The actual measurement frequency response is limited to 60 kHz because that is the natural freqency of the pressure ports in which the transducers are installed. The transducers are spaced 2.5 meters apart, sufficiently far to obtain a spatial picture of the pressure in the waveguide interior.

The facility utilizes two stainless steel tanks as indicated in Figure 1, both of which are made of stainless steel to prevent corrosion. Either the head tank, with a capacity of three gallons, or the drain tank, with a capacity of one gallon, can store the 20 kg of mercury in the system. The head tank holds 18.6 kilograms of mercury per inch of height, minimizing pressure fluctuations in the system from the flow of mercury to the drain tank. The drain tank has a capacity of 11.8 kilograms of mercury per inch, maximizing the mercury available to cover the suction line to the transfer pump. Both tanks have lexan lids that permit visual monitoring of the level of mercury in each tank. Each lid is equipped with a penetration for a Survivair HEPA filter whose purpose is to filter mercury vapor from air displaced in the tank as mercury flows from one tank to another. All other leak paths for air, such as tubing penetrations in the lids and the seams where the lids rest on the tanks, are sealed.

In an effort to remove air from the system when the waveguide is being filled with mercury, a vacuum pump is used to evacuate air from the waveguide before it is filled with mercury. If air is present in the waveguide during testing, experimental results will be distorted by the presence of additional compressibility in the system. In order to preclude the exhaust of mercury vapors into the atmosphere, the vacuum pump discharges into a HEPA filter.

Because the system contains mercury, a hazardous material, it is important that it not leak. The ends of the waveguide are sealed by means of flanged fittings. All tubing connections use compression fittings. The pump inlet and outlet fittings are NPT thread to Swagelock compression fitting adapters. The threads are sealed by means of teflon tape. The system contains seven valves. These valves are packless and are connected to the rest of the system through compression fittings. The mercury transfer pump is a diaphragm pump, which is without a moving seal surface to eliminate leakage. The hydraulic accumulators have threaded adapters connecting them to the system that are sealed by means of neoprene rubber o-rings. Drip pans have been placed below the experimental equipment to contain potential mercury leaks.

Waveguide Operating Procedures

Preoperational checks
Procedure 1 – Filling the drain tank
Procedure 2 – Transferring Hg from the drain tank to the head tank.
Procedure 3 – Filling the waveguide
Procedure 4 – Draining the waveguide to the drain tank
Procedure 5 – Draining the head tank to the drain tank
Procedure 6 – Circulating Hg through the waveguide with the mercury transfer pump
Procedure 7 –Data collection methodology
Procedure 8 - Replacing the impact diaphragm
Procedure 9 - Replacing the reflection coupon
Procedure 10 – Replacement of vacuum pump oil
Procedure 11 - Mercury spill cleanup procedure.

Preoperational checks:

Check for leaks.
Ensure that the impact diaphragm been replaced since the last data set was taken.
Check solenoid piston alignment.
Check system pressure.
Check valve lineup.
Verify that safety equipment (safety glasses, latex gloves, respirator) are on hand.

Procedure 1 – Filling the drain tank

1. Health and Safety must be on site to monitor mercury vapor in the air.
2. If the mercury vapor levels in the air are above established limits, the person performing this procedure must wear proper respirator protection.
3. Remove cap C1.
4. Insert funnel in tube.
5. Pour Hg in the funnel, taking care not to overflow the funnel.
6. When all of the Hg has been poured into the drain tank, remove the funnel and store in a container marked "Mercury Contaminated Equipment."
7. Reinstall cap C1.

Procedure 2 – Transferring Hg from the drain tank to the head tank

Valve positions, given in Figure 2, are

V1	Shut	V7	Shut
V2	Open	V8	Shut
V3	Shut	V9	Shut
V4	Open	V10	Open
V5	Shut	V11	Shut
V6	Open		

1. Check the drain tank level to ensure that it is between one-fourth and one-half full.
2. Check the vacuum pump oil level. If it is above or below the sightglass, replace the oil in accordance with Procedure 10.
3. Check that the vacuum pump is plugged in and that its ball valve is shut.
4. Turn on the vacuum pump.
5. Open the vacuum pump ball valve.
6. Verify that the vacuum pump pressure/vacuum gage shows greater than 29 inches of mercury vacuum. If not, shut off the vacuum pump and check the tightness of the compression fitting connecting the vacuum line the vacuum pump.
7. Slowly open V3. The vacuum shown on the gage will dip as the vacuum pump draws a suction on the waveguide. Verify that the vacuum returns to greater than 29 inches of mercury. Then shut the vacuum pump ball valve, turn off the vacuum pump, and monitor vacuum for two minutes. If vacuum does not remain above 29 inches, check for leaks in the system. The most likely source of leaks in the system is the flanges where the reflection coupons and impact diaphragms are located. They may not have been properly aligned when last worked on.
8. Once vacuum has held at greater than 29 inches for two minutes, open V11 to draw mercury into the transfer pump suction line to prime the pump.
9. Open V7
10. Turn on the transfer pump.
11. Listen for cavitation noise. If it persists for greater than one minute, turn off the mecury transfer pump and reprime.
12. Check the drain tank to ensure that Hg is circulating in the drain tank.
13. Throttle open V9 to transfer Hg to the head tank. Throttle V7 as necessary to ensure flow to the head tank.
14. When the mercury transfer pump begins to cavitate again, shut V6 and fully open V7.
15. Turn off the transfer pump.
16. Shut V11, V7, and V9.

Procedure 3 – Filling the waveguide

Valve positions, given in Figure 2, are

V1	Shut	V7	Shut
V2	Shut	V8	Shut
V3	Shut	V9	Shut
V4	Shut	V10	Shut
V5	Shut	V11	Shut
V6	Shut		

1. Check the vacuum pump oil level. If it is above or below the sightglass, replace the oil in accordance with Procedure 10.
2. Check that the vacuum pump is plugged in and that its ball valve is shut.
3. Turn on the vacuum pump.
4. Open the vacuum pump ball valve.
5. Verify that the vacuum pump pressure/vacuum gage shows greater than 29 inches of mercury vacuum. If not, shut off the vacuum pump and check the tightness of the compression fitting connecting the vacuum line the vacuum pump.
6. Slowly open V3. The vacuum shown on the gage will dip as the vacuum pump draws a suction on the waveguide. Verify that the vacuum returns to greater than 29 inches of mercury. Then shut the vacuum pump ball valve, turn off the vacuum pump, and monitor vacuum for two minutes. If vacuum does not remain above 29 inches, check for leaks in the system. The most likely source of leaks in the system is the flanges where the reflection coupons and impact diaphragms are located. They may not have been properly aligned when last worked on.
7. Once vacuum has held at greater than 29 inches for two minutes, open V1 to draw mercury into the waveguide from the head tank. Shut V8.

Procedure 4 – Draining the waveguide to the drain tank

Valve positions, given in Figure 2, are

V1	Shut	V7	Shut
V2	Shut	V8	Shut
V3	Shut	V9	Shut
V4	Open	V10	Open
V5	Shut	V11	Shut
V6	Open		

1. Open V2, V5 and V11 to drain low points in the waveguide.

Procedure 5 – Draining the head tank to the drain tank

Valve positions, given in Figure 2, are

V1	Shut	V7	Shut
V2	Shut	V8	Shut
V3	Shut	V9	Shut
V4	Shut	V10	Shut
V5	Shut	V11	Shut
V6	Shut		

1. Open V11 and V8 to drain Hg from the head tank.
2. When the drain tank level has stopped rising, shut V8 and V11.

Procedure 6 – Circulating Hg through the waveguide with the mercury transfer pump

Valve positions, given in Figure 2, are

V1	Shut	V7	Shut
V2	Shut	V8	Open
V3	Shut	V9	Open
V4	Open	V10	Open
V5	Shut	V11	Shut
V6	Open		

1. Turn on the mercury transfer pump.
2. Monitoring gages G1 and G2, throttle V6 and V10 to adjust the flowrate through the waveguide to the desired level.

Procedure 7 –Data collection methodology

1. Chose an impact diaphragm and reflection coupon. Install them in the waveguide in accordance with Procedures 8 and 9.
2. Check the head tank level. If it is empty, transfer mercury from the drain tank to the head tank in accordance with Procedure 2.
3. Fill the waveguide in accordance with Procedure 3.
4. Align the solenoid plunger with the impact diaphragm.
5. Activate the Virtual Bench Oscilloscope on the data acquisition computer.
6. Circulate mercury through the waveguide in accordance with Procedure .
7. Attempt a few impacts with the plunger, monitoring the oscilloscope.
8. When the oscilloscope trace remains consistent for five impacts, shut off the mercury transfer pump.
9. Collect data on ten impacts with the oscilloscope window set at 10 milliseconds. Widen the window to 100 milliseconds and collect data on one impact.
10. Turn on the mercury transfer pump.
11. Throttle V6 and V9 to obtain a desired differential pressure across the waveguide as shown on gages G1 and G2.
12. Collect data on ten impacts with the oscilloscope window set at 10 milliseconds. Widen the window to 100 milliseconds and collect data on one impact.
13. Repeat steps 11 and 12 for as many differential pressures are desired.
14. Turn off the mercury transfer pump
15. Drain the waveguide in accordance with Procedure 4.
16. Move Transducer 2 from port 3 to port 2.
17. Repeat steps 3 to 15.
18. Move Transducer 2 from port 2 to port 2.
19. Select another impact diaphragm and repeat the procedure.

Procedure 8 - Replacing the impact diaphragm

1. If this is the first time the procedure is performed, have health and safety on site to monitor the mercury vapor level in the air. If the mercury vapor level is above established limits, a gas mask must be worn for the duration of the procedure.
2. Verify that a catch basin is installed beneath the flange to be unbolted in order to catch any mercury leakage. If it is not already installed, install it now.
3. Drain the waveguide in accordance with Procedure 4.
4. Pull back the solenoid from flange F2.
5. Remove the bolts from F2.
6. Remove F2 and the impact diaphragm.
7. Install the new impact diaphragm.
8. Reinstall F2 and tighten the bolts.
9. Place the solenoid up against flange F2.

Note – If a rubber diaphragm is used, two sheets of 1/16-inch diaphragm rubber must be used. If a stainless steel diaphragm is used, it must have a minimum thickness of 0.010 inch. Additionally, to ensure proper sealing of the stainless steel diaphragm, it must be sandwiched between two rubber gaskets.

Note – If the impact diaphragm shows deformation, it must be disposed of as mercury contaminated waste. If it is undamaged, it must be stored in a container for mercury contaminated materials.

Note – Latex gloves must be worn during this procedure.

Procedure 9 - Replacing the reflection coupon

1. If this is the first time the procedure is performed, have health and safety on site to monitor the mercury vapor level in the air. If the mercury vapor level is above established limits, a gas mask must be worn for the duration of the procedure
2. Verify that a catch basin is installed beneath the flange to be unbolted in order to catch any mercury leakage. If it is not already installed, install it now.
3. Drain the waveguide in accordance with Procedure 4.
4. Remove the bolts from flange F1.
5. Remove F1 and the reflection coupon.
6. Install new reflection diaphragm.
7. Reinstall F1 and tighten bolts.

Note – If a stainless steel coupon is used, it must be sandwiched between two rubber gaskets.

Note – Mercury contaminated coupons must be stored in a container for mercury contaminated materials.

Note – Latex gloves must be worn during this procedure.

Procedure 10 – Replacement of vacuum pump oil

1. Ensure that V3 and the vacuum pump ball valve are shut.
2. Disconnect the vacuum pump from the vacuum line.
3. Align the vacuum pump drain plug over a container labeled as "Mercury Contaminated Vacuum Pump Oil."
4. Open the fill plug. Open the drain plug and drain the oil into the container, taking care to avoid spillage.
5. When no more oil comes out, shut the drain plug and put a lid on the waste oil container.
6. Add new oil to the vacuum pump until the oil level is half-way up the sightglass.
7. Connect the vacuum pump to the vacuum line

Procedure 11 - Mercury spill cleanup procedure.

1. Any spill clean-up will be monitored by a respresentative from Health and Safety.
2. If minor Hg spillage occurs, scoop up the spill and place mercury in a jar with a lid labeled "Contaminated Hg."
3. If major Hg spillage occurs, evacuate the lab and contact health and safety.

Note: Any spill of less than two quarts is a minor spill. Any spill of more than two quarts is a major spill.

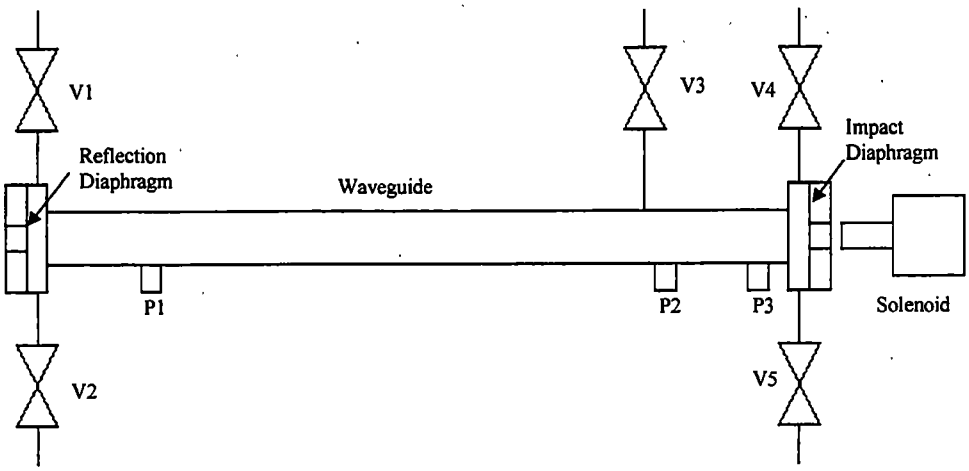


Figure 1 – Drawing of the waveguide

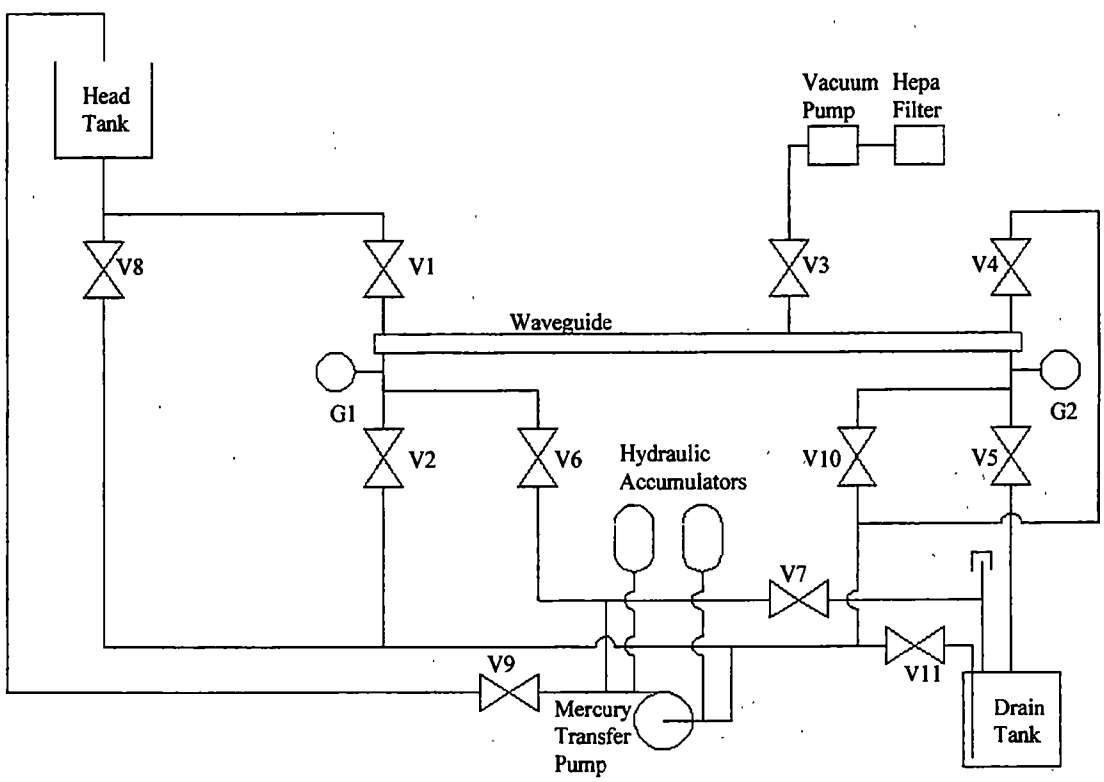


Figure 2 – Drawing of the waveguide piping system

APPENDIX I

DOCUMENTATION OF DATA

When a parameter on the waveguide (impact diaphragm, reflection coupon, flow conditions) is changed, 10 data files are taken with a 10 ms time window in order to obtain a high resolution picture of the behavior of the incident and reflected pressure pulses. One data file is taken with a 100 ms time window for a long-term view of the behavior of the system. The settings in Virtual Bench are described below:

(1) Time base – 1 ms per division

(2) Trigger – Normal

(3) Trigger Noise Rejection – 500 mV

(4) Data Samples – 5k

The default trigger location is adequate. The trigger noise rejection above refers to a triggering tool in Virtual Bench. When the trigger is set to normal, a multiple peak trace can be improperly measured. For example, if a trace has two peaks, at 2 ms and at 13 ms and it is desired to obtain information over the 0 to 10 ms time window, the trigger noise rejection must be set higher than the magnitude of the second peak. Otherwise, the trigger will be activated both at the first and second peaks. Only the trace from the most recent trigger is recorded. Usually, a Trigger Noise Rejection setting of 500 mV is adequate.

The naming of a data set is described below. When water was in the system, each case was named "Water Waveguide X" where X is a number. The first case was Water Waveguide 1. The second was Water Waveguide 2. The last case was Water Waveguide 38. The files representing the 10 ms time window are named "Water Waveguide – X – N" where N represents the Nth data file taken within that case. For example, the first data file of Water Waveguide 1 would be Water Waveguide – 1 – 1. The tenth data file

would be Water Waveguide – 1 – 10. The 100 ms data file of Water Waveguide 20 is Water Waveguide – 20 – Full Range, where "Full Range" represents a time base that shows the response of the system from initiation of a pressure pulse until the effects are no longer detectible. The same naming convention is used for data taken with mercury in the system. However, "Water Waveguide" has been replaced with "Mercury Waveguide." The lists of cases and the parameters used for each case are shown in Table I-1.

The first four cases with water in the waveguide were taken before the vacuum pump was installed in the system. The pressure traces change significantly from one data file in the case to another. Consequently, these cases are considered unreliable. Water cases 5 and 6 were taken after the vacuum pump was installed, but the triggering was not coherent.

The cases for mercury in the waveguide are listed in Table I-2. It must be noted that for cases 1, 2 and 3, there are no data files representing the 100 ms time window. The time base was inadvertently set at 1 s, instead of 100 ms. Hence, each case has a data file representing a 1 s time window.

Table I-1 – Parameters Used For Cases With Water In The Waveguide

Case	Parameters
1	Rubber impact diaphragm, rubber coupon, no flow in waveguide, transducer 1 in port P1, transducer 2 in port P3, 150 data files of 10 ms time window.
2	Rubber impact diaphragm, rubber coupon, no flow in waveguide, transducer 1 in port P1, transducer 2 in port P3, 99 data files of 10 ms time window.
3	Rubber impact diaphragm, rubber coupon,, no flow in waveguide, transducer 1 in port P1, transducer 2 in port P3, 3 lb/in spring on solenoid, 99 data files of 10 ms time window.
4	Rubber impact diaphragm, 0.4-inch stainless steel coupon (blind flange), no flow in waveguide, transducer 1 in port P1, transducer 2 in port P3, 99 data files of 10 ms time window.
5	Rubber impact diaphragm, 0.002-inch stainless steel coupon, no flow in waveguide, transducer 1 in port P1, transducer 2 in port P3. 100 data files of 10 ms time window.
6	Rubber impact diaphragm, 0.003-inch stainless steel coupon, no flow in waveguide, transducer 1 in port P1, transducer 2 in port P3, 100 data files of 10 ms time window.
7	Rubber impact diaphragm, 0.001-inch stainless steel coupon, no flow in waveguide, transducer 1 in port P1, transducer 2 in port P3, 100 data files of 10 ms time window.

Table I-1 – Parameters Used For Cases With Water In The Waveguide (Continued)

Case	Parameters
8	Rubber impact diaphragm, 0.005-inch stainless steel coupon, no flow in waveguide, transducer 1 in port P1, transducer 2 in port P3, 100 data files of 10 ms time window.
9	Rubber impact diaphragm, rubber coupon, no flow in waveguide, transducer 1 in port P1, transducer 2 in port P3, 99 data files of 10 ms time window.
10	Rubber impact diaphragm, 0.063-inch stainless steel coupon, no flow in waveguide, transducer 1 in port P1, transducer 2 in port P3, 78 data files of 10 ms time window.
11	Rubber impact diaphragm, 0.4-inch stainless steel coupon (blind flange), no flow in waveguide, transducer 1 in port P1, transducer 2 in port P3, 25 data files of 10 ms time window.
12	Rubber impact diaphragm, 0.025-inch stainless steel coupon, no flow in waveguide, transducer 1 in port P1, transducer 2 in port P3, 100 data files of 10 ms time window.
13	Rubber impact diaphragm, 0.020-inch stainless steel coupon, no flow in waveguide, transducer 1 in port P1, transducer 2 in port P3, 99 data files of 10 ms time window.
14	Rubber impact diaphragm, rubber coupon, 37 psid across waveguide, transducer 1 in port P1, transducer 2 in port P3, 100 data files of 10 ms time window.

Table I-1 – Parameters Used For Cases With Water In The Waveguide (Continued)

Case	Parameters
15	Rubber impact diaphragm, rubber coupon, 12 psid across waveguide, transducer 1 in port P1, transducer 2 in port P3, 100 data files of 10 ms time window.
16	Rubber impact diaphragm, 0.020-inch stainless steel coupon, 37 psid across waveguide, transducer 1 in port P1, transducer 2 in port P3, 100 data files of 10 ms time window.
17	Rubber impact diaphragm, 0.020-inch stainless steel coupon, 12 psid across waveguide, transducer 1 in port P1, transducer 2 in port P3, 100 data files with 10 ms time window.
18	Rubber impact diaphragm, 0.025-inch stainless steel coupon, no flow in waveguide, transducer 1 in port P1, transducer 2 in port P3, 100 data files with 10 ms time window, 1 data file with 100 ms time window.
19	Rubber impact diaphragm, 0.025-inch stainless steel coupon, 12 psid across waveguide, transducer 1 in port P1, transducer 2 in port P3, 100 data files with 10 ms time window, 1 data file with 100 ms time window.
20	Rubber impact diaphragm, 0.025-inch stainless steel coupon, 37 psid across waveguide, transducer 1 in port P1, transducer 2 in port P3, 100 data files with 10 ms time window, 1 data file with 100 ms time window.
21	0.010-inch stainless steel impact diaphragm, 0.025-inch stainless steel coupon, no flow in waveguide, transducer 1 in port P1, transducer 2 in port P3, 10 data files with 10 ms time window, 1 data file with 100 ms time window.

Table I-1 – Parameters Used For Cases With Water In The Waveguide (Continued)

Case	Parameters
22	0.010-inch stainless steel impact diaphragm, 0.025-inch stainless steel coupon, 12 psid across waveguide, transducer 1 in port P1, transducer 2 in port P3, 10 data files with 10 ms time window, 1 data file with 100 ms time window.
23	0.010-inch stainless steel impact diaphragm, 0.025-inch stainless steel coupon, 37 psid across waveguide, transducer 1 in port P1, transducer 2 in port P3, 10 data files with 10 ms time window, 1 data file with 100 ms time window.
24	0.015-inch stainless steel impact diaphragm, 0.025-inch stainless steel coupon, no flow in waveguide, transducer 1 in port P1, transducer 2 in port P3, 10 data files with 10 ms time window, 1 data file with 100 ms time window.
25	0.015-inch stainless steel impact diaphragm, 0.025-inch stainless steel coupon, 12 psid across waveguide, transducer 1 in port P1, transducer 2 in port P3, 10 data files with 10 ms time window, 1 data file with 100 ms time window.
26	0.015-inch stainless steel impact diaphragm, 0.025-inch stainless steel coupon, 37 psid across waveguide, transducer 1 in port P1, transducer 2 in port P3, 10 data files with 10 ms time window, 1 data file with 100 ms time window.
27	0.020-inch stainless steel impact diaphragm, 0.025-inch stainless steel coupon, no flow in waveguide, transducer 1 in port P1, transducer 2 in port P3, 10 data files with 10 ms time window, 1 data file with 100 ms time window.

Table I-1 – Parameters Used For Cases With Water In The Waveguide (Continued)

Case	Parameters
28	0.020-inch stainless steel impact diaphragm, 0.025-inch stainless steel coupon, 12 psid across waveguide, transducer 1 in port P1, transducer 2 in port P3, 10 data files with 10 ms time window, 1 data file with 100 ms time window.
29	0.020-inch stainless steel impact diaphragm, 0.025-inch stainless steel coupon, 37 psid across waveguide, transducer 1 in port P1, transducer 2 in port P3, 10 data files with 10 ms time window, 1 data file with 100 ms time window.
30	0.025-inch stainless steel impact diaphragm, 0.025-inch stainless steel coupon, no flow in waveguide, transducer 1 in port P1, transducer 2 in port P3, 10 data files with 10 ms time window, 1 data file with 100 ms time window.
31	0.025-inch stainless steel impact diaphragm, 0.025-inch stainless steel coupon, 12 psid across waveguide, transducer 1 in port P1, transducer 2 in port P3, 10 data files with 10 ms time window, 1 data file with 100 ms time window.
32	0.025-inch stainless steel impact diaphragm, 0.025-inch stainless steel coupon, 37 psid across waveguide, transducer 1 in port P1, transducer 2 in port P3, 10 data files with 10 ms time window, 1 data file with 100 ms time window.
33	0.063-inch stainless steel impact diaphragm, 0.025-inch stainless steel coupon, no flow in waveguide, transducer 1 in port P1, transducer 2 in port P3, 10 data files with 10 ms time window, 1 data file with 100 ms time window.

Table I-1 – Parameters Used For Cases With Water In The Waveguide (Continued)

Case	Parameters
34	0.063-inch stainless steel impact diaphragm, 0.025-inch stainless steel coupon, 12 psid across waveguide, transducer 1 in port P1, transducer 2 in port P3, 10 data files with 10 ms time window, 1 data file with 100 ms time window.
35	0.063-inch stainless steel impact diaphragm, 0.025-inch stainless steel coupon, 37 psid across waveguide, transducer 1 in port P1, transducer 2 in port P3, 10 data files with 10 ms time window, 1 data file with 100 ms time window.
36	0.063-inch stainless steel impact diaphragm, 0.025-inch stainless steel coupon, no flow in waveguide, transducer 1 in port P1, transducer 2 in port P2, 10 data files with 10 ms time window, 1 data file with 100 ms time window.
37	0.063-inch stainless steel impact diaphragm, 0.025-inch stainless steel coupon, 12 psid across waveguide, transducer 1 in port P1, transducer 2 in port P2, 10 data files with 10 ms time window, 1 data file with 100 ms time window.
38	0.063-inch stainless steel impact diaphragm, 0.025-inch stainless steel coupon, 37 psid across waveguide, transducer 1 in port P1, transducer 2 in port P2, 10 data files with 10 ms time window, 1 data file with 100 ms time window.

Table I-2 – Parameters Used For Cases With Mercury In The Waveguide

Case	Parameters
1	0.025-inch stainless steel impact diaphragm, 0.063-inch stainless steel coupon, no flow in waveguide, transducer 1 in port P1, transducer 2 in port P3, 10 data files with 10 ms time window, 1 data file with 1 s time window.
2	0.025-inch stainless steel impact diaphragm, 0.063-inch stainless steel coupon, 45 psid across waveguide, transducer 1 in port P1, transducer 2 in port P3, 10 data files with 10 ms time window, 1 data file with 1 s time window.
3	0.025-inch stainless steel impact diaphragm, 0.063-inch stainless steel coupon, 80 psid across waveguide, transducer 1 in port P1, transducer 2 in port P3, 10 data files with 10 ms time window, 1 data file with 1 s time window.
4	0.025-inch stainless steel impact diaphragm, 0.063-inch stainless steel coupon, no flow in waveguide, transducer 1 in port P1, transducer 2 in port P2, 10 data files with 10 ms time window, 1 data file with 100 ms time window.
5	0.025-inch stainless steel impact diaphragm, 0.010-inch stainless steel coupon, no flow in waveguide, transducer 1 in port P1, transducer 2 in port P2, 10 data files with 10 ms time window, 1 data file with 100 ms time window.
6	0.025-inch stainless steel impact diaphragm, 0.010-inch stainless steel coupon, no flow in waveguide, transducer 1 in port P1, transducer 2 in port P3, 10 data files with 10 ms time window, 1 data file with 100 ms time window.

Table I-2 – Parameters Used For Cases With Mercury In The Waveguide (Continued)

Case	Parameters
7	0.010-inch stainless steel impact diaphragm, 0.010-inch stainless steel coupon, no flow in waveguide, transducer 1 in port P1, transducer 2 in port P3, 10 data files with 10 ms time window, 1 data file with 100 ms time window.

APPENDIX J

TIME OF FLIGHT

Theoretical sound speeds in the waveguide were calculated for three separate boundary conditions by means of Equations [B-37], [B-38] and [B-39]. It was desired to determine the boundary condition most applicable to the waveguide. Additionally, the measured sound speed can serve as an indication of air in the waveguide. A liquid-gas phase sound speed is lower than the liquid-phase sound speed. Each case is represented by a number of data files. For all of the mercury cases, there were ten data files representing each case. All ten files in each case were analyzed. For water cases 21 through 38, ten data files represented each case. As in the mercury cases, all ten files in each case were analyzed. Water cases 6 through 21 are represented by nominally one hundred data files, with a few exceptions. The first ten data files of each case were analyzed.

The time of flight are determined by using a half magnitude method. The maximum and minimum points on the leading edge of a pressure pulse detected at transducer port 1 are measured. Then, the two measurements are averaged. This average value is located on the leading edge of the pulse, and the time associated with that point is recorded. This process is repeated on the leading edge of the same pressure pulse when it is detected at transducer port 2 (or 3, whichever is in use). The difference between the two times is taken to determine the time of flight between transducer ports 1 and 2 (or 3). The distance between transducer ports P1 and P2 (or P3) is divided by this time delay to obtain the sound speed. The transducer port locations and the distances between them are shown in Figure 1.

Table J-1 – Sound Speed Associated With Each Water Case

Case Number	Sound Speed		
	Average	Maximum	Minimum
6	1384	1390	1390
7	1429	1435	1424
8	1384	1392	1348
9	1439	1448	1430
10	1436	1444	1429
11	1430	1441	1408
12	1430	1443	1418
13	1437	1446	1428
14	1449	1454	1448
15	1445	1450	1443
16	1473	1478	1466
17	1442	1449	1436
18	1445	1455	1438
19	1458	1469	1450
20	1452	1464	1440
21	1438	1448	1433
22	1435	1437	1434
23	1435	1438	1434
24	1438	1440	1434
25	1437	1438	1435

Table J-1 – Sound Speed Associated With Each Water Case (Continued)

Case Number	Sound Speed		
	Average	Maximum	Minimum
26	1436	1438	1433
27	1441	1443	1437
28	1437	1438	1433
29	1437	1440	1433
30	1438	1442	1433
31	1434	1436	1430
32	1438	1440	1433
33	1478	14823	1475
34	1426	1429	1422
35	1424	1429	1397
36	1418	1423	1411
37	1347	1429	1296
38	1391	1464	1336

Table J-2 – Sound Speed Associated With Each Mercury Case

Case Number	Sound Speed		
	Average	Maximum	Minimum
1	1162	1164	1160
2	1165	1177	1154
3	1087	1139	988
4	1085	1176	1032
5	1094	1125	1070
6	1035	1041	1027
7	1104	1108	1092

APPENDIX K

PICTURES OF WAVEGUIDE

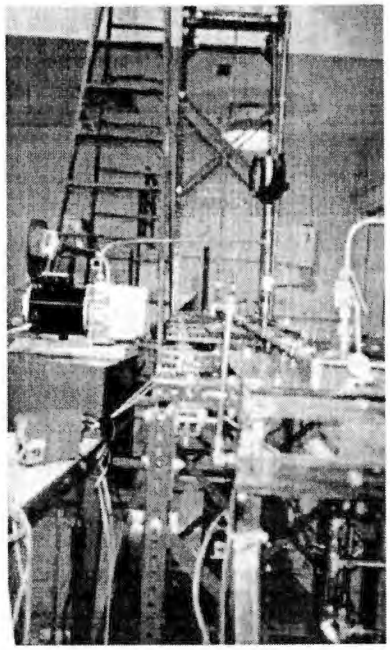


Figure K-1 – Waveguide and Vacuum Pump

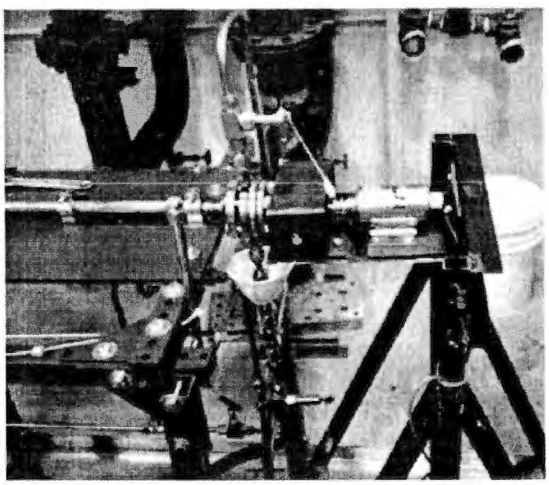


Figure K-2 – Solenoid and Impact Diaphram

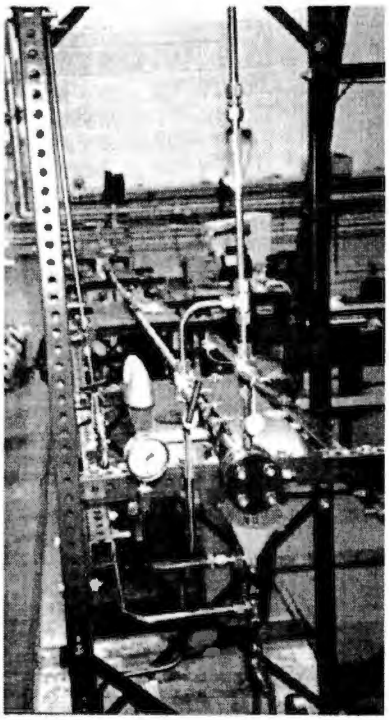


Figure K-3 – Reflection Coupon

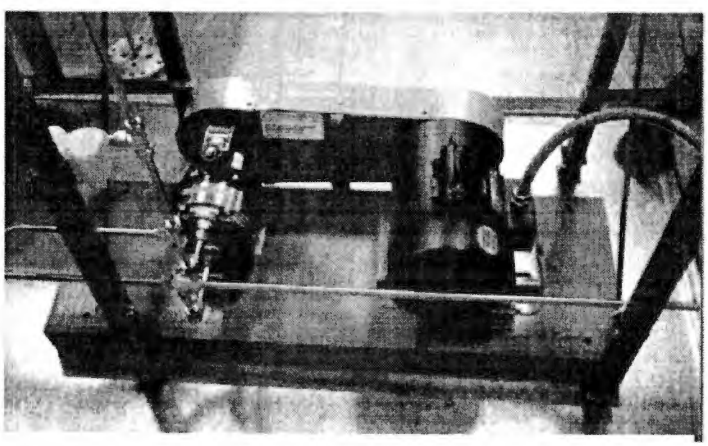


Figure K-4 – Mercury Transfer Pump

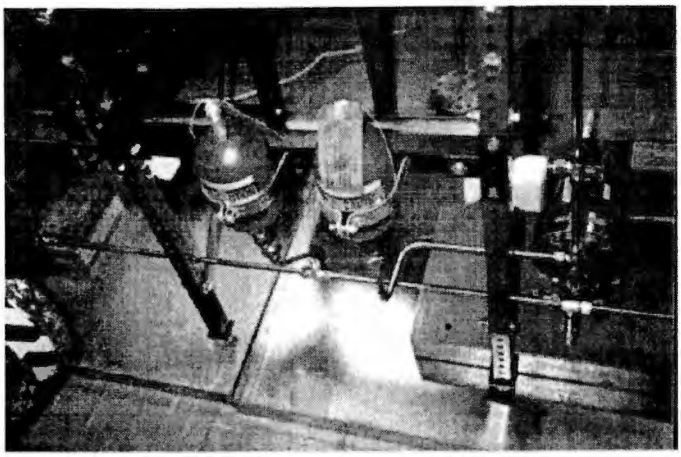


Figure K-5 – Hydraulic Accumulators

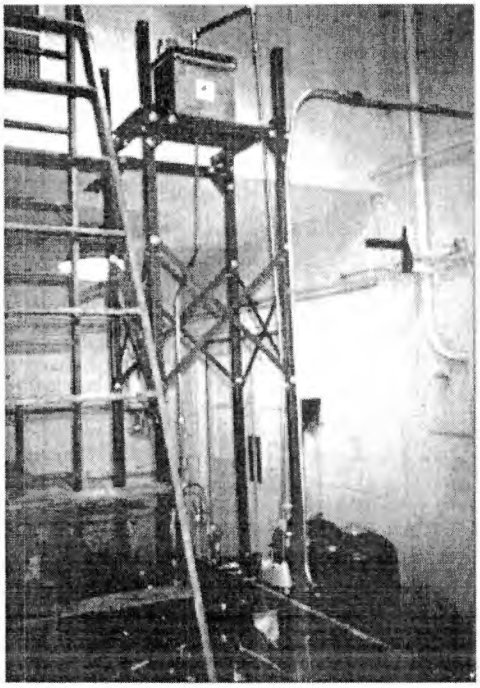


Figure K-6 – Head Tank

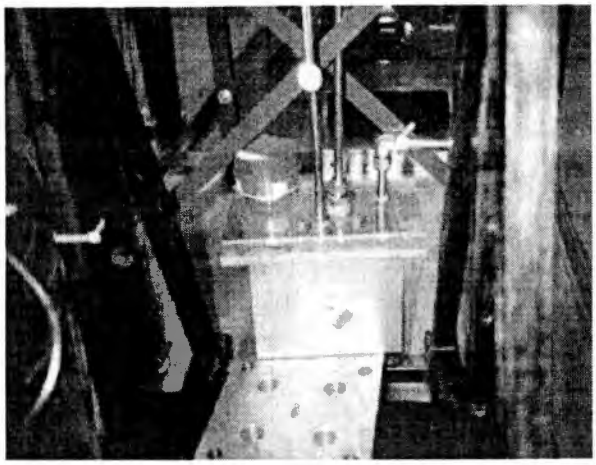


Figure K-7 – Drain Tank

NOMENCLATURE

A	Acceleration
a	Radius of a branch line
B_T	Bulk modulus
c	Sound speed
C	Damping coefficient
C_f	Pressure drop coefficient
c_p	Specific heat at constant pressure
c_v	Specific heat at constant volume
$d()/d(t)$	Total derivative with respect to time, or other selected variable
$\partial()/\partial(t)$	Partial derivative with respect to time, or other selected variable
$\delta()$	Finite change, larger than a differential change
D	Diameter
D_h	Hydraulic diameter
e	Wall thickness
E	Elastic modulus
f	Force
f	Frequency
f	Friction factor
F	Force
f_n	Natural frequency
g	Gravitational acceleration
h	Height
H	Height of a fluid column
k	Wavelength constant
k_s	Stiffness coefficient
l	Length of a Helmholz oscillator neck
l'	Effective length of a Helmholz oscillator neck
L	Length
m	Mass
m_g	Mass of gas in hydraulic accumulator
p	Pressure
P	Pressure
P_i	Incident pressure
P_r	Reflected pressure
P_0	Initial Pressure
p_b	Branch line pressure wave amplitude
p_i	Incident pressure wave amplitude
p_r	Reflected pressure wave amplitude
p_t	Transmitted pressure wave amplitude
Q	Heat
R	Acoustic resistance
R	Radius
Re	Reynolds number

s	Acoustic condensation
S	Cross-sectional area
S_b	Branch line cross-sectional area
t	Time
T	Temperature
v	Velocity
V	Volume
V	Rigid volume of a Helmholz oscillator
V_g	Volume of gas in hydraulic accumulator
W	Work
x	Position
X	Acoustic reactance
Z	Acoustic impedance
α	Attenuation constant
α_b	Branch coefficient of transmissivity
α_r	Coefficient of reflectivity
α_t	Coefficient of transmissivity
γ	Ratio of specific heats
Δl	End correction for a Helmholz oscillator neck
η	Shear coefficient of viscosity
μ	Poisson's ratio
ρ	Density
σ	Normal stress
τ	Stroke time of mercury transfer pump
υ	Specific volume
ϕ	Phase shift
ξ	Acoustic displacement
ω	Angular frequency
ω_0	Natural angular frequency

Vita

Rodney Harvill was born in Corinth, Mississippi on April 19, 1969. He attended schools in the public system of Madison County, Tennessee, where he graduated from North Side High School in June, 1987. He enlisted in the United States Navy in February of 1988 and was trained as a Machinists Mate in the Navy's Nuclear Power Program. After his discharge in January, 1994, he entered the University of Tennessee at Knoxville. He received a Bachelor of Science in Nuclear Engineering in May, 1997. During his undergraduate work, he worked at Oak Ridge National Laboratory and at Roadway Package Service. In June, 1997, he entered the Master's program in Nuclear Engineering at the University of Tennessee at Knoxville. The Master's degree was received December, 1998. In May, 1997, he married Allison Joelle Howard. He now works for Consumers Energy at the Palisades Nuclear Plant.